Report 2004.027

Interpretation of the Ra 3 potential field data along the Lofoten-Vøring continental margin, Part 2

NGU
Norges geologiske undersøkelse
Geological Survey of Norway

Geological Survey of Norway
N-7491 Trondheim, Norway
Tel.: 47 73 90 40 11
Telefax 47 73 92 16 20

REPORT

Report no.: 2004.027	ISSN 0800-3416	Grading: Confidential to 30.04.2009

Title:
Interpretation of the Ra 3 potential field data along the Lofoten-Vøring continental margin, Part 2

Authors:	Clients:
Odleiv Olesen, Jörg Ebbing, Erik Lundin, Jan Reidar Skilbrei, Mark A. Smethurst & Trond H. Torsvik	BP Norge, Norsk Hydro, Statoil, Oljedirektoratet and NGU

County:	Commune:
Nordland and Troms	
Map-sheet name (M=1:250.000)	Number of pages: 56 Price (NOK):
Mo I Rana, Bodø, Svolvær, Narvik and Andøya	Map enclosures:

Fieldwork carried out:	Date of report:	Project no.:	Person responsible:
May-July, 2003	30.04.2004	3025.00	Dypstein Nordgulen

Summary:

Aeromagnetic data from the Røst Basin (RAS-03) were acquired in 2003 and merged with 12 neighbouring datasets. A compilation of the existing gravity data in the area has also been carried out. Forward 3D modelling along 17 profiles is constrained by available data on density, magnetic properties and reflection and refraction (OBS) seismics. The new data show that the previously interpreted oceanic fracture zones (Gleipne, Surt, Bivrost, Jenegga and Vesterålen) do not exist. Apparent offsets in the oceanic spreading anomalies were caused by poor navigation and wide line spacing of the vintage datasets. Consequently, opening of the Norwegian-Greenland Sea between the Jan Mayen and Senja-Greenland fracture zones occurred along a stable axis without offsets of the oceanic spreading anomalies or jumps in spreading axis. Reconstruction of the East Greenland aeromagnetic data to Chron 22 (c. 47.7 Ma) reveals that a c. 50 km wide igneous complex cut across the spreading anomalies 24A, 24B and 23 from the Vøring Marginal High on the Norwegian margin to the Traill Ø on the East Greenland coast. The complex (refereed to as Traill Ø-Vøring igneous complex in the present report) links up with the NE-SW trending initial magmatic lineament (IML) between the Traill Ø and the Kangerlussuaq regions. The introduction of the Traill Ø-Vøring igneous complex simplifies the initial opening history and excludes the need to invoke the abandoned spreading ridge and the Gleipne Fracture Zone along the Vøring margin.

The 3D modelling of the potential field data reveals that the Surt Lineament is not a regional tectonic boundary separating basement rocks of different physical parameters. Combined interpretation of reflection seismic and potential field data in a seismic workstation environment show that the western half of the Røst Basin is heavily affected by intrusions (bearing resemblance to the dykes and sills in the Hel Graben). A basement structure map shows that the Sandflesa and Flakstad basement highs occur at depths of approximately 6 km in the Røst Basin. The former is dominated by mafic or ultramafic intrusions within the Myken volcanic complex. The transfer zones on the Lofoten margin are not spatially connected to younger oceanic fracture zones as previously interpreted.

The results of the Ra 3 Project show the importance of applying high-quality potential field data in conjunction with seismic data in regional tectonic studies.

Keywords: Geofysikk	Kontinentalsokkel	Tolkning
Berggrunnsgeologi	Magnetometri	Forkastning
Petrofysikk	Gravimetri	Fagrapport

CONTENTS

1. INTRODUCTION

The present study is a follow-up on the interpretation of the Røst Aeromagnetics Project 2003 (Ra 3) financed by BP Norge, Norsk Hydro, Statoil, the Norwegian Petroleum Directorate and the Geological Survey of Norway. The focus area of Part 1 of the Ra 3 Interpretation Report (Olesen et al. 2003) was the Utgard High - Sandflesa High - Utrøst Ridge - Røst Basin area. The present study area (Fig. 1.1) has been extended southwestwards along the Vøring margin to include:

1) A new aeromagnetic data compilation for the Vøring-Lofoten region (including the SPT-93, VGVB-94 and VBEAM-00 surveys).
2) Plate reconstruction for the Norwegian and Greenland Seas showing reconstructed aeromagnetic anomalies and interpreted features.
3) Combined 3D interpretation of the Surt Lineament.
4) An integrated study of seismic and aeromagnetic data in a seismic work station environment focusing on delineating sill intrusions and lava flows.

These tasks were prioritised by the Ra 3 steering committee during a project meeting in Trondheim on January 21, 2004.

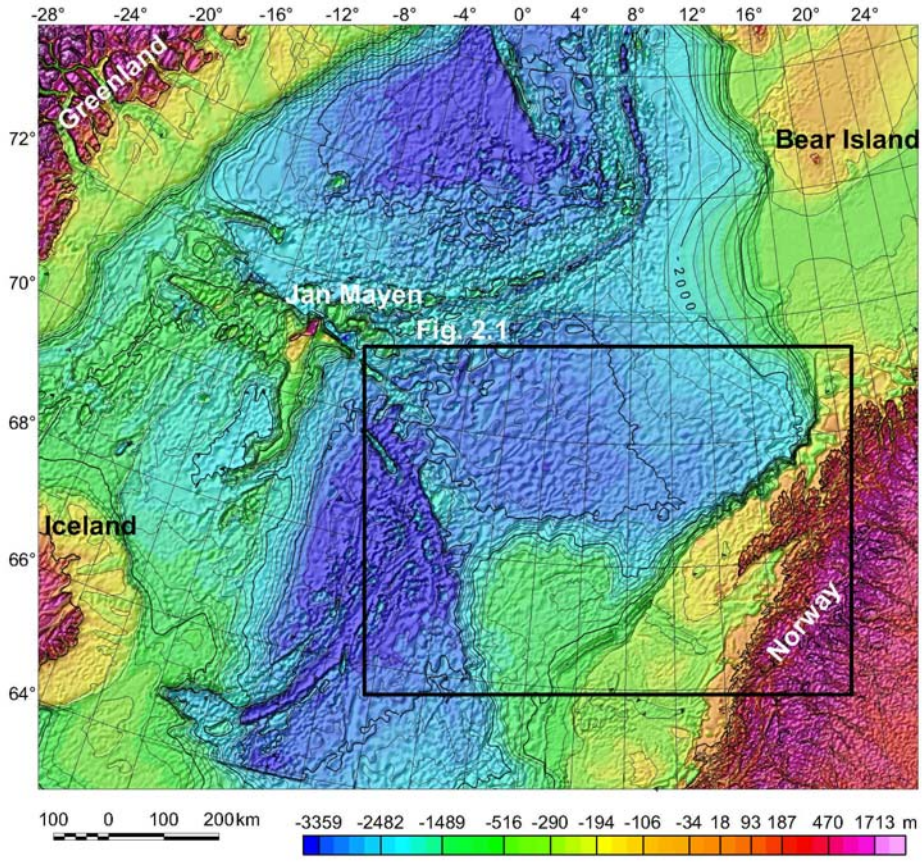

Figure 1.1 Bathymetry and topography, Norwegian and Greenland Seas, 200 and 1000 m contour intervals (modified from Dehls et al. 2000, Olesen et al. 2003). The black rectangle shows the map area of Fig. 2.3.

2. DATASETS

2.1 Aeromagnetic data

A total of 10 offshore aeromagnetic surveys (Fig. 2.1) have been compiled in the present project. Specifications for these surveys are shown in Table 2.1. Vintage data that were reflown in 1989, 1994, 1998 and 2003 are not included in the table, and are also excluded in the final map compilation. The pattern of flight lines generally provides data along NW-trending profiles with a spacing of 2-5 km. The LAS-89 (Olesen & Myklebust 1989), NAS-94 (Olesen & Smethurst 1995), VAS-98 (Mauring et al. 1999) and RAS-03 (Mauring et al. 2003) surveys have been processed within the Ra-3 project using the loop closure method (Mauring et al. 2003). The NGU-69 and NGU-73 surveys were reprocessed separately using the median levelling technique (Mauring et al. 2002) by Olesen et al. (2002). We have in the present new compilation included the SPT-93, VGVB-94 and VBE-AM-00 surveys. The acquisition and processing of the latter two surveys are described by Amarok (1995) and TGS-Nopec (2000), respectively. A smoothed grid version of the SPT-93 survey was included in the initial Ra 3 compilation (Olesen et al. 2003), while the present updated compilation includes a new SPT-93 grid calculated from the original profiles, without applying any smoothing. We have included the Gammaa5 grid by Verhoef et al. (1996) from the Norwegian-Greenland Seas (after a regridding of the 5x5 km grid to a grid consisting of 500x500 m cells). The Gammaa5 compilation includes the NRL-73 survey and several other aeromagnetic surveys offshore Greenland and Iceland, in addition to a large number of ship-lines in the southwestern part of our regional study area.

Table 2.1. Offshore aeromagnetic surveys compiled for the present study (Figs. 2.1 & 2.4). The RAS-03 survey included 2.300 km reflying of the LAS-89 survey.

Year	Area	Operator	Survey name	Navigation	Sensor elevation m	Line spacing km	Length km
1969	69º - 70ºN	NGU	NGU-69	Decca	200	4	1.000
1973	Vøring Basin	NGU	NGU-73	Loran C	500	5	6.000
1972 1973	Norwegian-Greenland Seas	Naval Research Lab.	NRL-73		300	10-20	45.000
1989	Lofoten	NGU	LAS-89	GPS/ Loran C/ Syledis	250	2	24.000
1993	Hel Graben-Nyk High	World Geo-science	SPT-93	GPS	80	0.75	19.000
1994	Nordland Ridge-Helgeland Basin	NGU	NAS-94	GPS	150	2	36.000
1994	Vøring Basin	Amarok	VGVB-94	GPS	140	1-3	31.800
1998	Vestfjorden	NGU	VAS-98	GPS	150	2	6.000
2000	Southern Gjallar Ridge	TGS-Nopec	VBEAM-00	GPS	130	1-4	17.000
2003	Røst Basin	NGU	RAS-03	GPS	230	2	30.000

Table 2.2 Aeromagnetic grids (500 x 500 m) included in the regional compilation. The Gammaa5 compilation (5 x 5 km grid) by Verhoef et al. (1996) from the Norwegian-Greenland Seas was regridded to a 500x500m grid and included in the regional compilation (Figs. 2.1 & 2.4).

Year	Area	Operator	Navigation	Sensor elevation	Line spacing km	Recording
1964	Andøya	NGU	Visual	150 m above ground	1	Analogue
1965	Vesterålen area	NGU	Visual	300 m above ground	2	"
1971-73	Nordland-Troms	NGU	Decca	1000 m above sea level	2	"

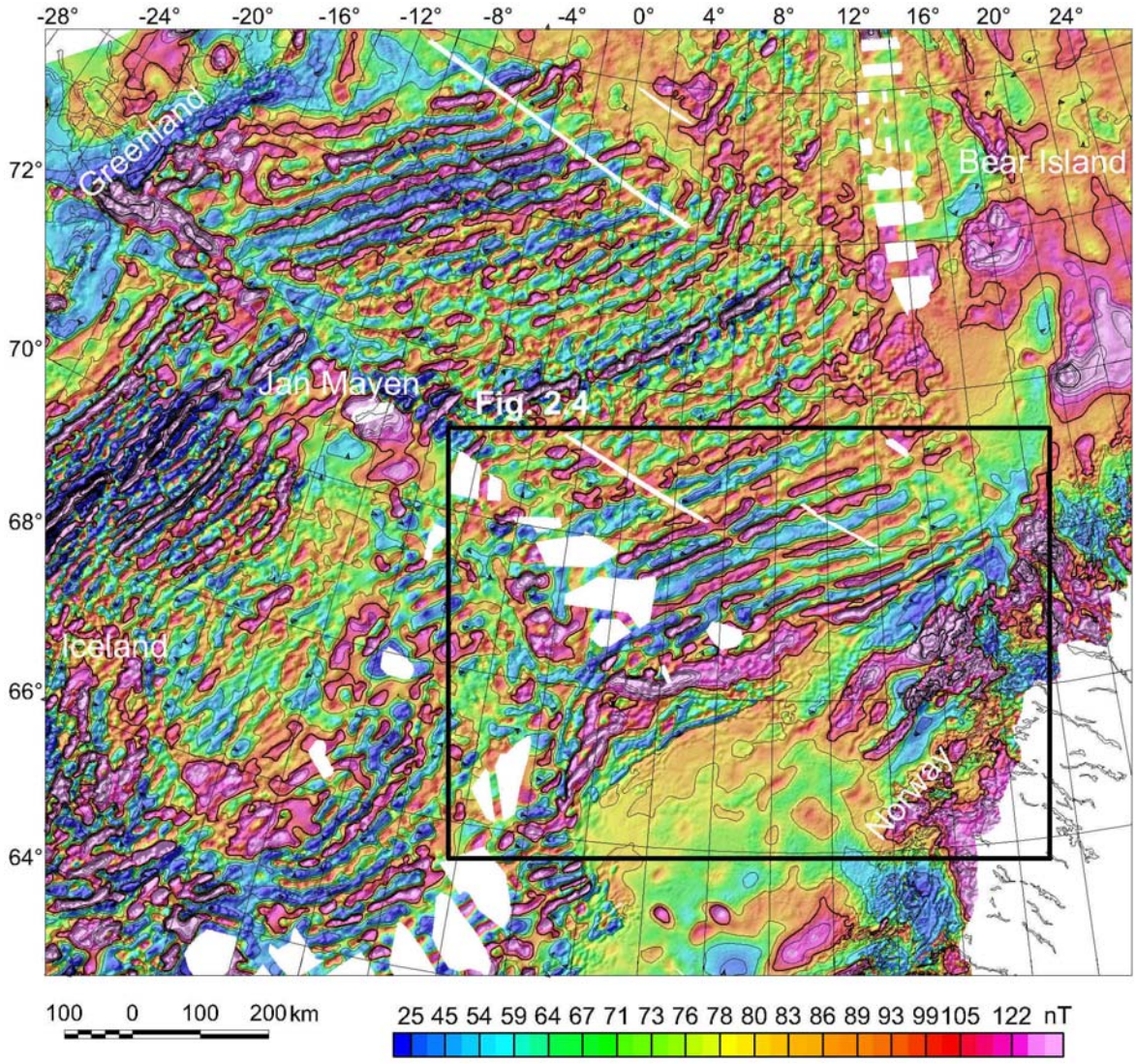

Figure 2.1 Compilation of aeromagnetic surveys (Tables 2.1 & 2.2) in the Norwegian and Greenland Seas. The black frame shows the Vøring-Lofoten continental margin area (Fig. 2.4).

Specifications for the different sub-areas are given in Tables 2.1 and 2.2. The grids were trimmed to c. 10 km overlap and merged using the minimum curvature algorithms, GRIDKNIT and GRIDSTICH, developed by Geosoft (2000a) and Desmond Fitzgerald and Associates (1996), respectively. The final grid shown in Fig. 2.1 and 2.4 was displayed using the shaded-relief technique with illumination from the southeast. To enhance the high frequency component of the compiled dataset a shaded relief version (in grey-tones) of the 20 km Gaussian high-pass filtered grid has been produced and superimposed on the coloured total field maps (Figs. 2.1 & 2.4). The contour intervals of the aeromagnetic maps are 20 nT (thin lines) and 100 nT (bold lines).

2.2 Gravity and petrophysical data

The compilation of Bouguer gravity grid is described by Olesen et al. (2003) in the Ra 3 Interpretation Report Part 1. An Airy-Heiskanen 'root' (Heiskanen & Moritz 1967) was calculated from a compiled topographic and bathymetric dataset (see Fig. 1.1 and section 2.4 in Olesen et al. (2003)). The gravitational attraction from the 'root' was calculated using the AIRYROOT algorithm (Simpson *et al.* 1983). The isostatic residual (Figs. 2.2 & 2.5) was achieved by subtracting the gravity response of the Airy-Heiskanen 'root' from the observed Bouguer gravity data. A 100 km Gaussian high-pass filtered map of the compiled Bouguer gravity dataset has also been produced and presented by Olesen et al. (2003). The shaded relief versions (in grey tones) of the high-pass filtered grid is superimposed on the gravity residual maps in Figs. 2.2 and 2.5. The contour intervals are 5 mGal (thin lines) and 20 mGal (bold lines).

The pronounced magnetic and gravimetric anomalies within the project are continuous from land onto the continental shelf (Figs. 2.1 – 2.5). It is important to know the density and magnetic properties of the rocks on land when interpreting the potential field data in the offshore area. Approximately 4700 rock samples collected during geological mapping and geophysical studies have been measured with respect to density, susceptibility and remanence. Statistical information on this dataset, in addition to magnetic properties of cored volcanics from the Ocean Drilling Program (ODP) and density data from petroleum exploration wells, was compiled by Olesen et al. (2003).

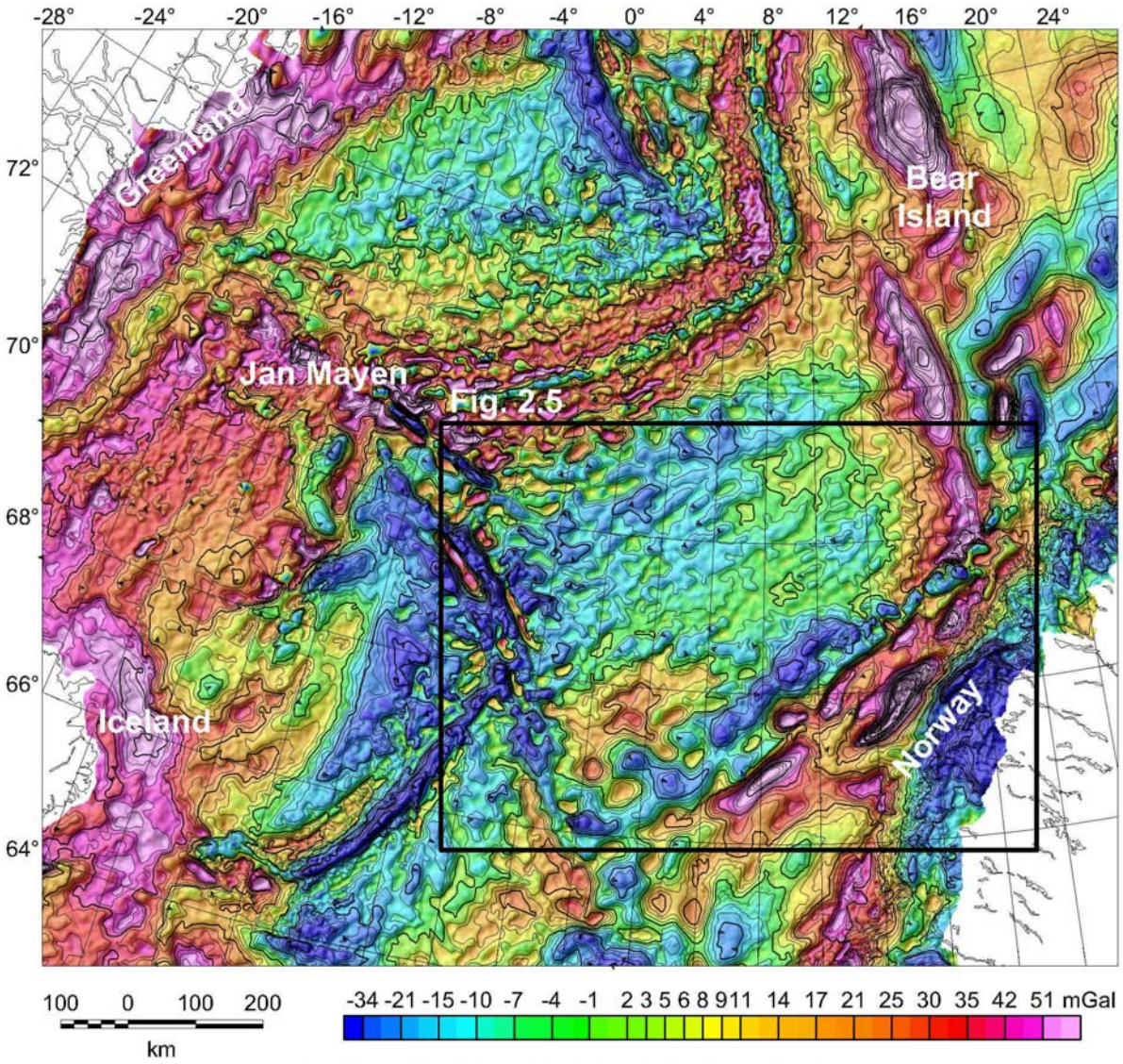

Figure 2.2 *Residual gravity after isostatic correction of Bouguer gravity data from the Greenland and Norwegian Seas and adjacent areas. The isostatic correction has been calculated applying the AIRYROOT algorithm (Simpson et al. 1983) to the topography/bathymetry in Fig. 1.1 (rock density 2670 kg/m^3 on land, 2200 kg/m^3 at sea and a crust/mantle density contrast of 300 kg/m^3). The black frame shows the map area of Fig. 2.5.*

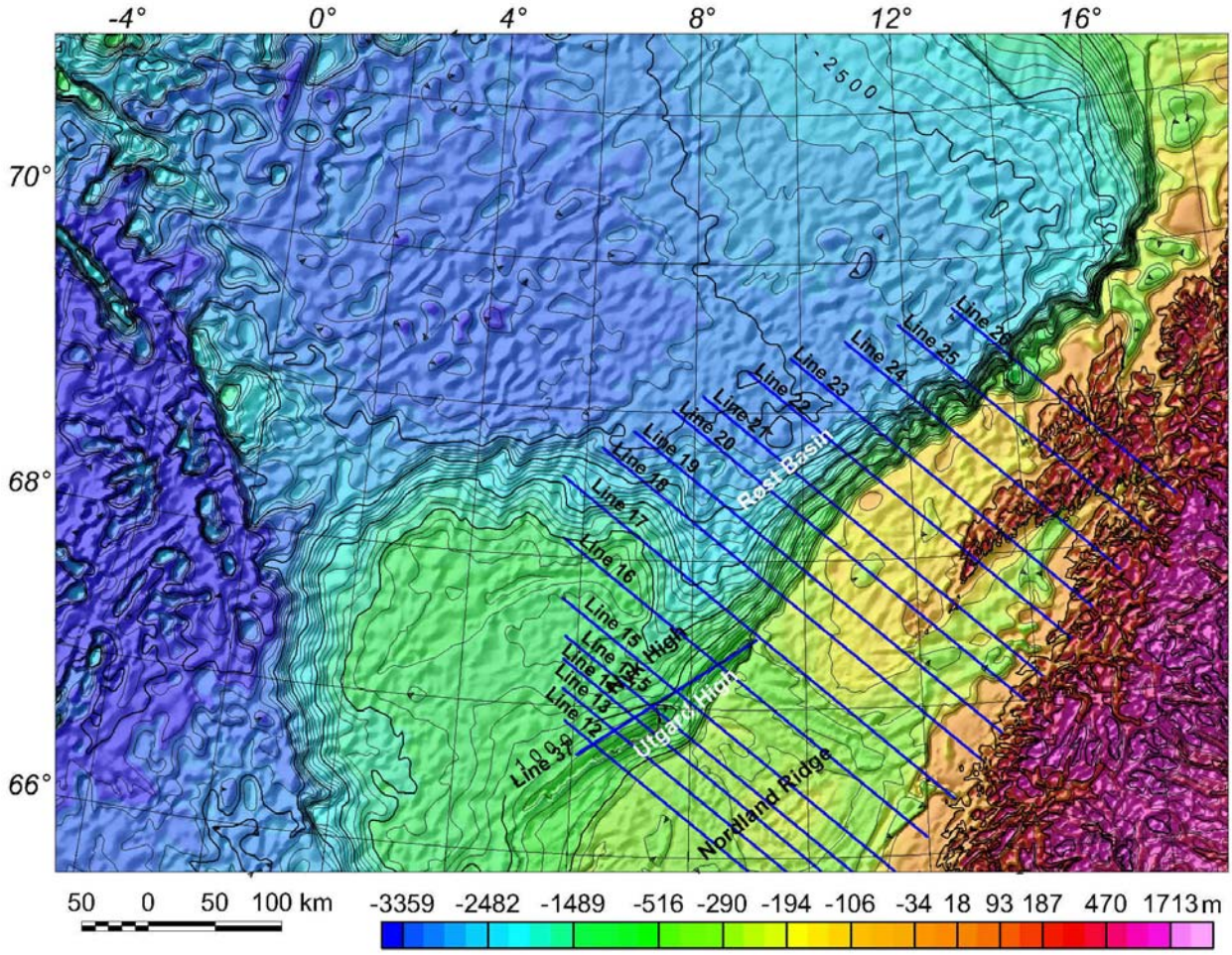

Figure 2.3 *Bathymetry and topography, Vøring – Lofoten continental margin area: Enlargement of Fig. 1.1. The blue lines show the interpreted sections within the 3D model. An updated version of the southern part of the model (Lines 12-15 and Crossline 37) is shown in the present report, while the northern part of the model is presented in Part 1 of the Ra 3 Project reports by Olesen et al. (2003).*

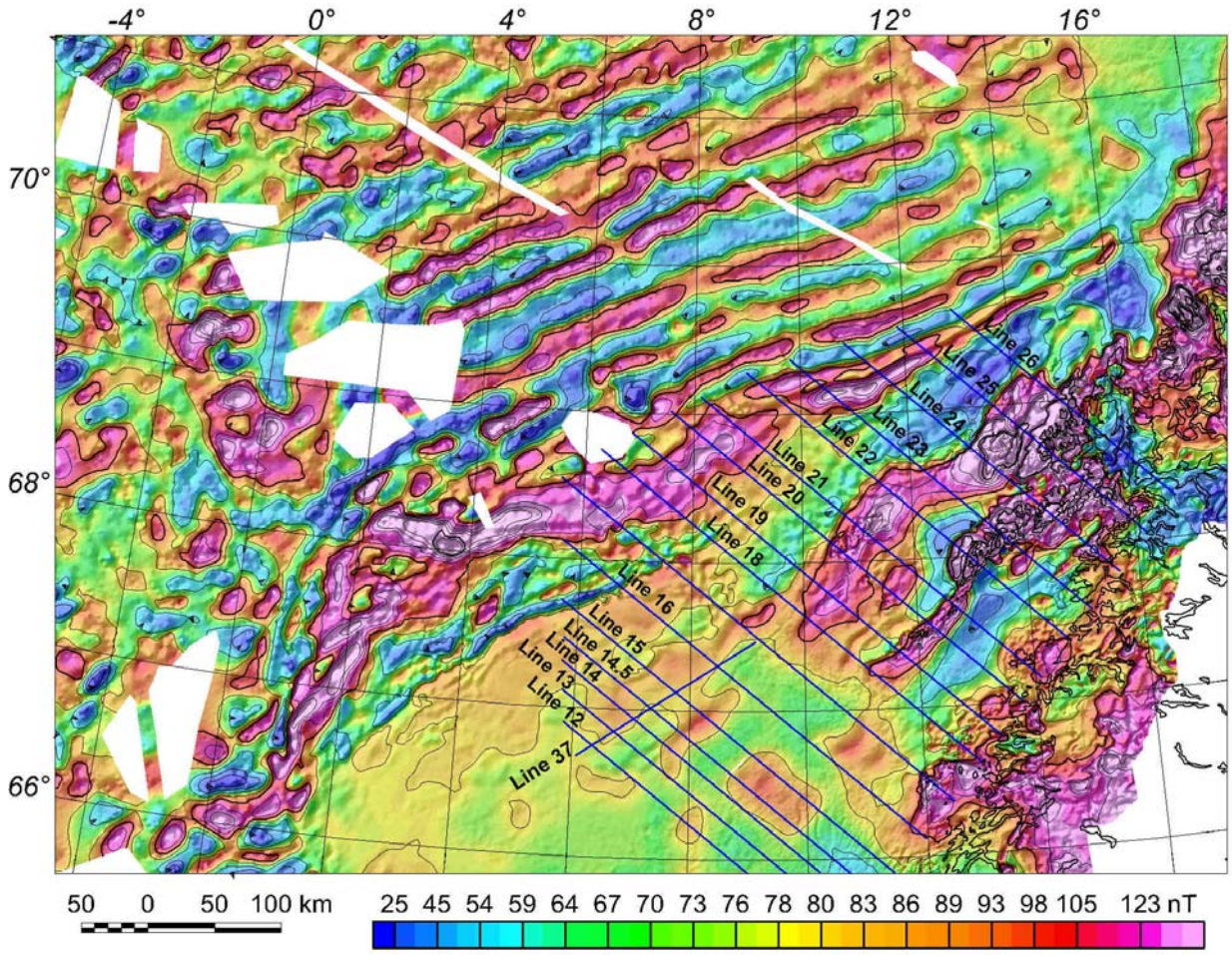

Figure 2.4 *Compilation of aeromagnetic surveys in the Nordland-Vøring area (enlargement of Fig. 2.1). The map includes the NRL-73 US Naval Research Laboratory 1973, VGVB-94 - Vertical Gradient Vøring Basin 1994, VBEAM-00 - Vøring Basin Extension Aeromagnetic Survey 2000, SPT-93 - Simon Petroleum Technology 1993, RAS-03 - Røst Aeromagnetic Survey 2003, LAS-89 - Lofoten Aeromagnetic Survey 1989, NAS-94 - Nordland Aeromagnetic Survey 1994 and VAS-1998 - Vestfjorden Aeromagnetic Survey 1998 (Tables 2.1 & 2.2). The latter four surveys were acquired by the Geological Survey of Norway. The blue lines show the interpreted sections within the 3D model.*

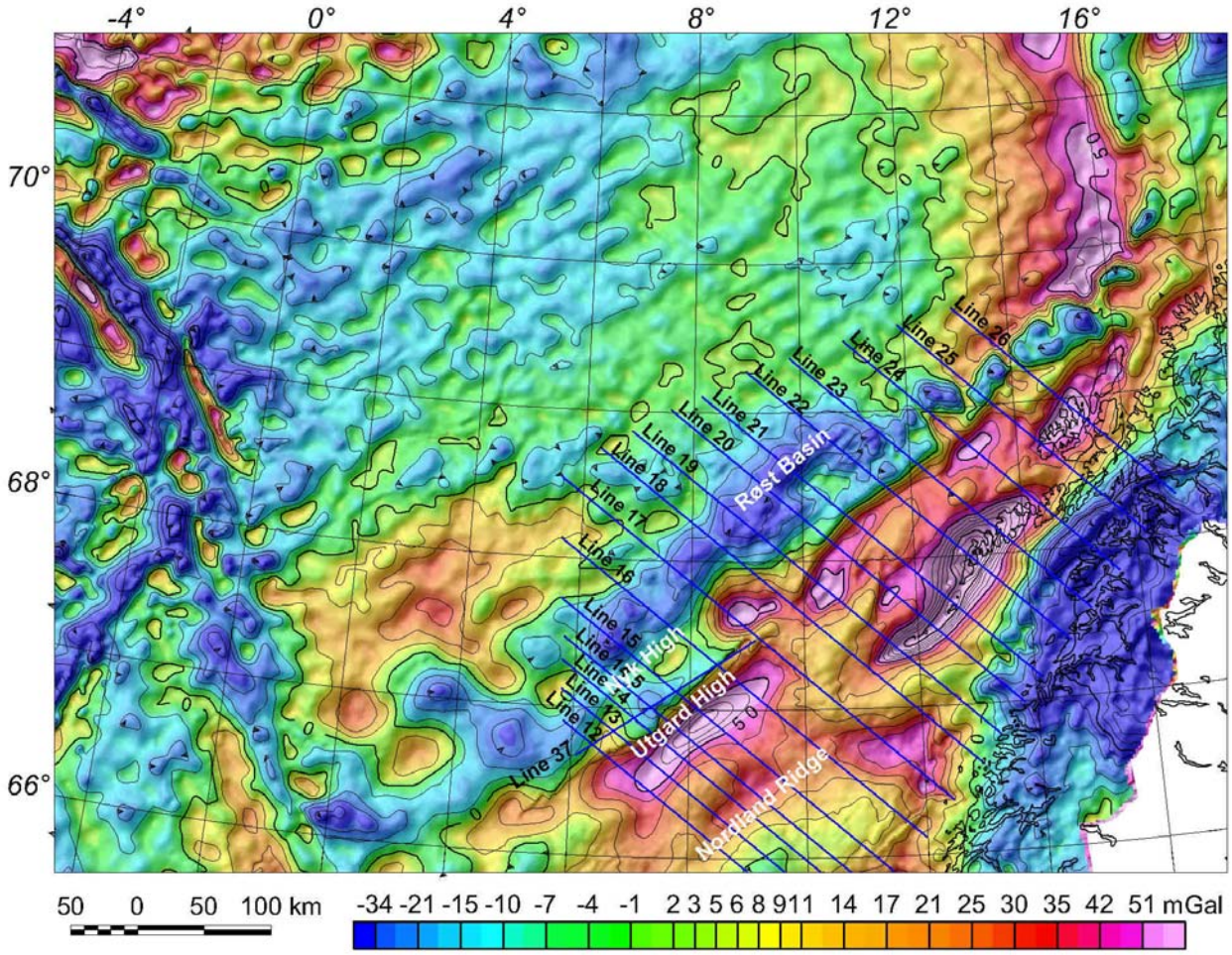

Figure 2.5 *Residual gravity after isostatic correction of Bouguer gravity data: Enlargement of Fig. 2.2.*

2.3 Seismic studies

In the area interpretations of Ocean Bottom Seismograph (OBS) arrays are available from the studies of Mjelde et al. (1992, 1993, 1997, 1998, 2002, 2003a,b,c). The results of the OBS arrays have been interpreted along profiles, providing a good coverage of the study area.

Further structural interpretations are available by Blystad et al. (1995). Brekke & Riis (1987), Brekke (2000), Eldholm et al. (2002), Berndt et al. (2000, 2001), Lundin & Doré (1997), Løseth & Tveten (1996), Skogseid et al. (1992) and Tsikalas et al. (2001, 2002) present additional interpretations from reflection seismic profiles along the margin. The information of these studies was considered, wherever possible, to constrain the modelling and analysis results.

3. INTERPRETATION METHODS

3.1 Data presentation and geophysical interpretation map

Aeromagnetic and gravity maps at a scale of 1:500.000 were included in the Ra 3 Interpretation Report Part 1. Histogram-equalised colour, high-frequency filtered and shaded-relief images were produced to enhance the information of the regional datasets. The maps were also presented in A3 format. Similar maps are produced of the extended datasets that are compiled in the present study (Part 2 of the Ra 3 Project).

The grid datasets were analysed with the Oasis Montaj software (Geosoft 2000b, 2001). Fault zones within the basement, and partly within the sediments, were interpreted from the aeromagnetic map (Olesen et al. 2003). The faults are plotted on Figs. 5.6 – 5.9. High frequency anomalies representing volcanic rocks are also included. These anomalies are often negative. The interpreted location of the easternmost boundary of the flow basalts (Blystad et al. 1995, Tormod Henningsen pers. comm. 2003) in the Vøring and Røst basins is added to the geophysical maps. The combined interpretation of depth estimates from both gravity and aeromagnetic data was carried out by interpolation and contouring of depth to basement by Olesen et al. (2003) and shown in Figs. 5.7 & 5.8.

Aeromagnetic grid and structural elements on the Greenland continental margin have been rotated back to Europe (Fig. 3.1) using the rotation algorithms by Cox & Hart (1986) and the rotation parameters in Table 3.1.

Table 3.1. Euler rotation parameters used to restore Greenland back to its 49.7 and 54.0 Ma positions relative to Europe.

Age (Ma)	Mag. anomaly	Period	Latitude	Longitude	Angle	Recording
49.7	22	L. Ypresian	52.7	125.5	9.8	Interpolated from Mosar et al. (2002)
54.0	24	E. Ypresian	65.3	111.8	15.4	Present study

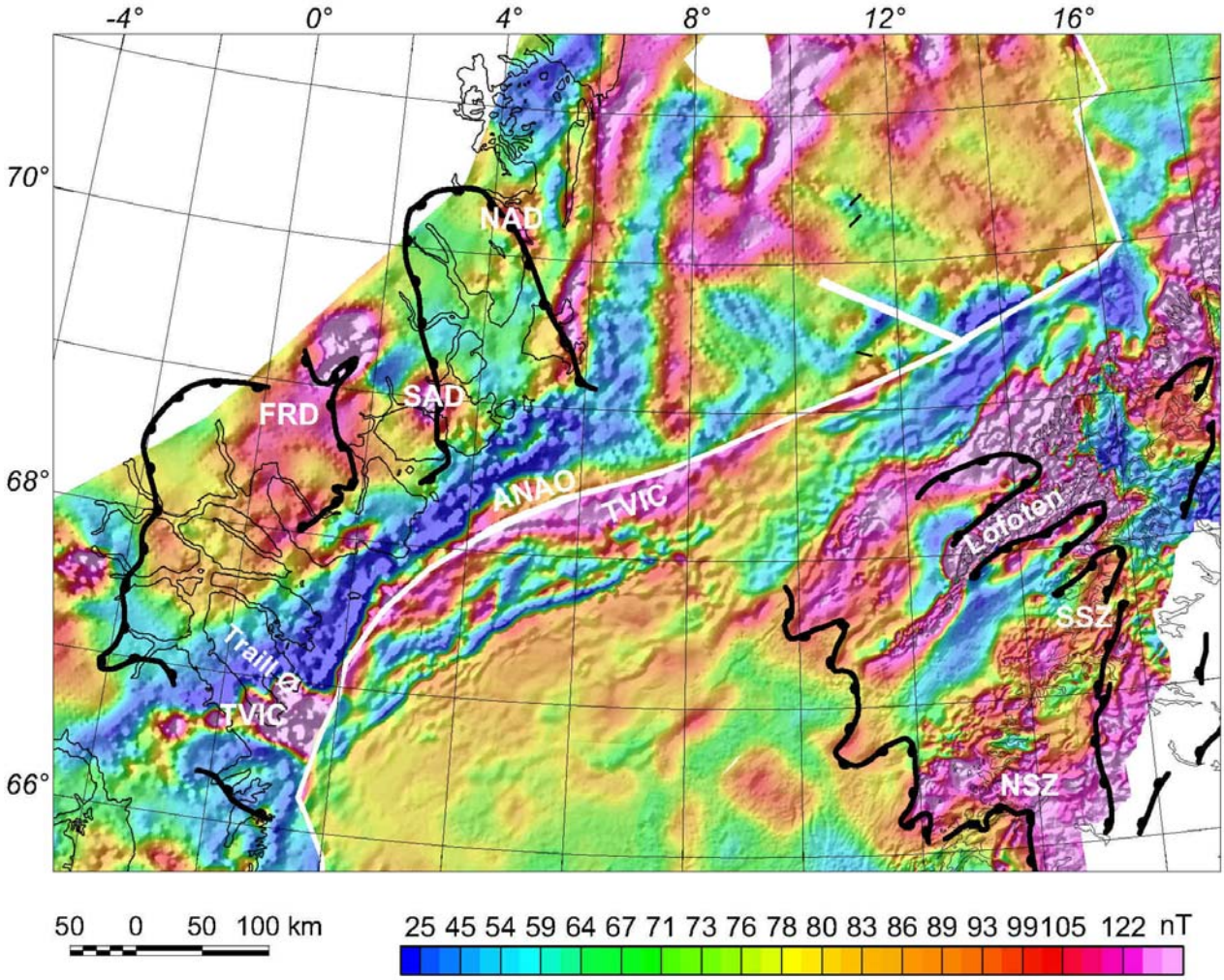

Figure 3.1 *Restoration of the Greenland aeromagnetic grid to its former position relative to Norway at the time of opening of the Norwegian and Greenland Seas (c. 54 Ma). Note that parts of the younger Traill Ø - Vøring igneous complex (TVIC) are left in the continental crust on either side of original continent-ocean boundaries after restoration. The bold black lines show late Caledonian detachment zones of Hartz et al. (2002), Braathen et al. (2002) and Olesen et al. (2002). ANAO – Axis of North Atlantic opening; SSZ – Sagfjord Shear Zone; NSZ – Nesna Shear Zone; NAD – Northern Ardencaple Fjord Detachment; SAD – Southern Ardencaple Fjord Detachment; FRD – Fjord Region Detachment system.*

3.2 Joint interpretation of seismic and potential field data (on Geoframe Charisma workstation)

The seismic data and the potential field data were loaded into a seismic workstation in the premises of the Norwegian Petroleum Directorate (NPD). The GeoQuest software Geoframe Charisma Imain, running on a Unix workstation, was applied to interpret the datasets. Total magnetic field data, high-pass filtered magnetic data, as well as gravity data, have been plotted on top of seismic sections crossing the 'inner flows' as shown in Fig. 5.17. Seismic lines crossing the Røst Basin and the Vøring Escarpment were analysed. Examples of selected

lines are presented in Fig. 5.18 – 5.21. The objective of the study was to analyse the intrasedimentary volcanic rocks, seen as high-amplitude seismic reflectors, and their relation to short-wavelength magnetic anomalies within the Røst Basin. In particular, we wanted to see if the anomalies that occur to the north and west of the 'inner flows' are due to flows or intrusions.

3.2.1 3D modelling

The 3D forward modelling of the gravity and magnetic fields has been carried out with the modelling software IGMAS (Interactive Gravity and Magnetic Application Software: Götze & Lahmeyer 1988, Schmidt & Götze 1998, Breunig et al. 2000).

The model of the Nordland area is mainly based on the density model of Olesen et al. (2002) and references therein. Applied density estimates of sediments and basement and magnetic properties of volcanic rocks in the Vøring area were displayed in Table 2.4 and 2.6 of the Ra 3 Part 1 Report (Olesen et al. 2003). The Moho topography and lower crustal densities have been deduced from published OBS seismic data (Mjelde et al. 1992, 1993, 1997, 1998, 2002, 2003a,b,c).

The model consists of 16 parallel cross-sections in the study area with a distance of 20-35 km (Figs. 2.3 - 2.5 and 5.8 - 5.9). In addition, the model was extended 5000 km in each direction to avoid edge effects. In the central part of the model the location of the lines coincides with the location of the OBS profiles presented by Mjelde et al. (1992). The five southernmost sections are presented in Figs 5.11 – 5.15 while the others are shown as Figs. 5.4 – 5.13 in the Ra 3 Report, Part 1 by Olesen et al. (2003).

4. STRUCTURAL FRAMEWORK

The general evolution of the NE Atlantic seafloor spreading and the rifting history has been described at length elsewhere (e.g. Doré et al. 1999, Roberts et al. 1999, Lundin 2002) and is not repeated here. Fig. 4.1 shows the main offshore structure elements along the Vøring-Lofoten margin (from Blystad et al. 1995).

The first Ra 3 report provided evidence against the presence of oceanic fracture zones off the Lofoten margin (cf. Tsikalas et al. 2002, in press). In this report we question the common interpretation of the Gleipne Fracture Zone shown in Fig. 4.4 (e.g. Hagevang et al. 1983, Skogseid & Eldholm 1987, Blystad et al. 1995, Gerignon et al. 2003) as well as the interpretation of an abandoned spreading ridge off the SW Vøring margin (Hagevang et al. 1983). Thus, the Ra 3 Project has resulted in a much simpler early seafloor spreading architecture on the Norwegian

margin than what is commonly suggested in the literature. It appears reasonable to assume that the early seafloor of the conjugate Greenland margin is equally simple.

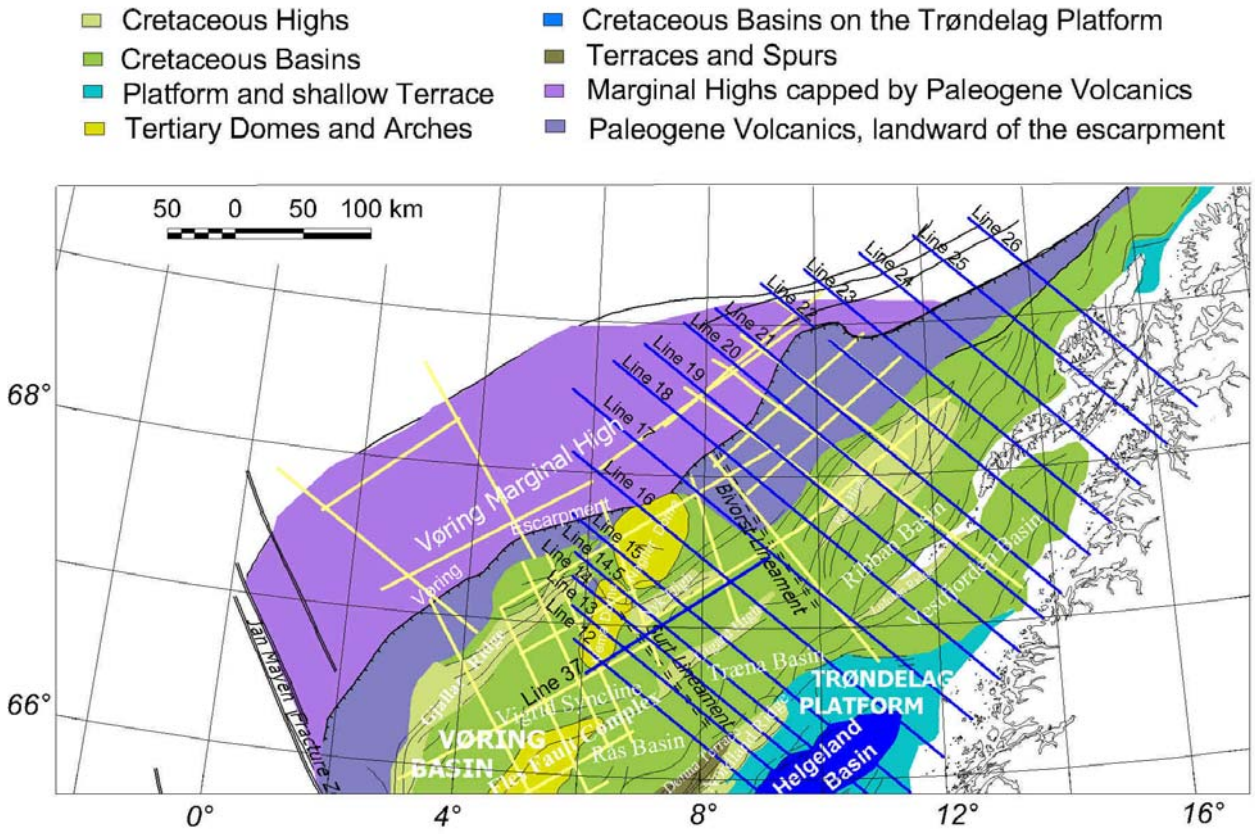

Figure 4.1 *Main structural elements along the Vøring-Lofoten continental margin (modified from Blystad et al. 1995). Yellow lines show OBS lines by Mjelde et al. (1992, 1993, 1997, 1998, 2001, 2003a,b,c). Blue lines depict interpretation lines within the 3D model. Lines 12-15 are presented in the present report while Lines 16-28 are presented in the Ra 3 Part 1 report (Olesen et al. 2003).*

Another contribution of this report is the distinction of the broad, diffuse, and high amplitude anomalies along the Vøring margin, West Jan Mayen Fracture Zone, and the southern NE Greenland margin. These anomalies are distinctly different from the narrow and comparatively simple seafloor spreading anomalies further north. By accepting different origins of the mentioned anomalies, there is no need to invoke complicated offsets or repetitions of the magnetic anomalies as previously proposed.

More detailed descriptions of the late Caledonian orogenic collapse were covered in the first RA-3 report. Of particular interest is the recognition of the structurally denuded basement culminations onshore Norway, and their bounding detachments. These major detachments formed during orogen-parallel extension and hence trend at a high angle to the orogen (Fig. 4.2 and 5.6 - 5.10). Similar age and style detachments are mapped in E Greenland (Hartz et al. 2002). Even if the central part of the orogen has been segmented during the episodic Late Phanerozoic and Mesozoic rifting, the presence of detachments of similar age and style on both conjugate margins suggest that the detachments exist offshore. Indeed, the Norwegian detachments have been traced

offshore (Olesen et al. 2002). The entire Mid Norway-East Greenland crystalline basement is still affected by a NW-SE structural grain generated during Late Palaeozoic NE-SW trending extension. Precise correlation between the shear zones in E Greenland and Norway (Olesen et al. 2003) is probably speculative since the degree of lateral relative motion between the continents during Devonian time remains uncertain.

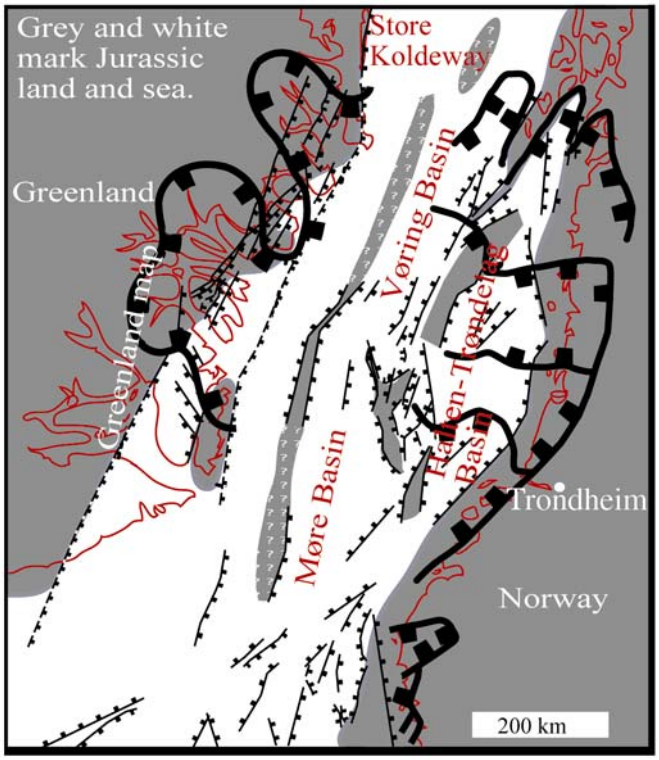

Figure 4.2 *Sketch map of the main structural elements in the Norwegian-Greenland Sea area before opening of the Atlantic (modified from Hartz et al. 2002, Braathen et al. 2002, Olesen et al. 2002, Skilbrei et al. 2002).*

Extrapolating the onshore structures to the offshore realm, it can be deduced that the area outboard of Nordland experienced NE-trending (i.e. orogen-parallel) late Caledonian gravity collapse. The Kollstraumen detachment and Nesna and Sagfjord shear zones (Figs. 4.2 and 5.7) (Osmundsen et al. 2003) extend northwestwards below the Helgeland, Vestfjorden and Ribban basins (Olesen et al. 2002). The Bivrost Lineament is interpreted to represent a detachment dipping 5-15º to the southwest and may constitute the offshore extension of the Nesna shear zone. While the Bivrost Lineament represents a major Mesozoic structural boundary between the Vøring Basin and Lofoten margin, it is clear that the lineament rejuvenated a much older zone of crustal weakness (the mentioned Devonian detachment), which was also suggested by Mokhtari & Pegrum (1992). Downfaulted low-magnetic Caledonian nappes are interpreted to constitute the "basement" southwest of the Bivrost Lineament. The offshore extension of the Sagfjord shear zone may have governed the location of the large-scale Mesozoic normal fault zones that bound the sides of the Lofoten and Utrøst Ridges (Olesen et al. 2003).

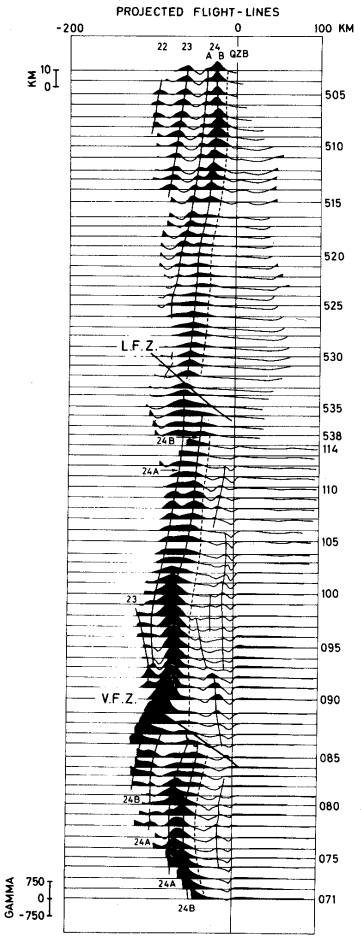

A)

Figure 4.3 Interpretation of magnetic spreading anomalies along the Vøring-Lofoten margin (Hagevang et al. 1983). A) Stacked profiles of the NGU-73 aeromagnetic data. Note that the anomalies across the Lofoten and Vøring Fracture Zones (LFZ and VFZ) can alternatively be interpreted as continuous anomalies (without any offset). The uniform amplitude and wavelength of the anomalies do in fact support this interpretation (the Vøring fracture zone has later been referred to as the Gleipne Fracture Zone by Blystad et al. (1995)). B) Regional interpretation of oceanic spreading anomalies and fracture zones. Note the suggested abandoned spreading ridge just outboard of the SW Vøring margin.

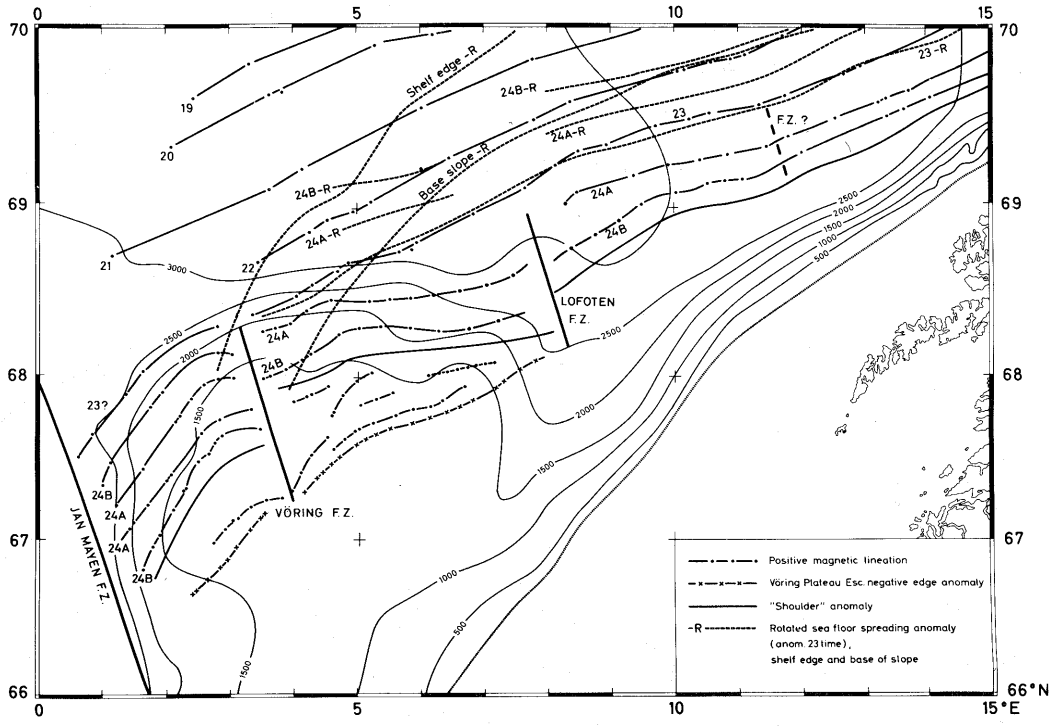

B)

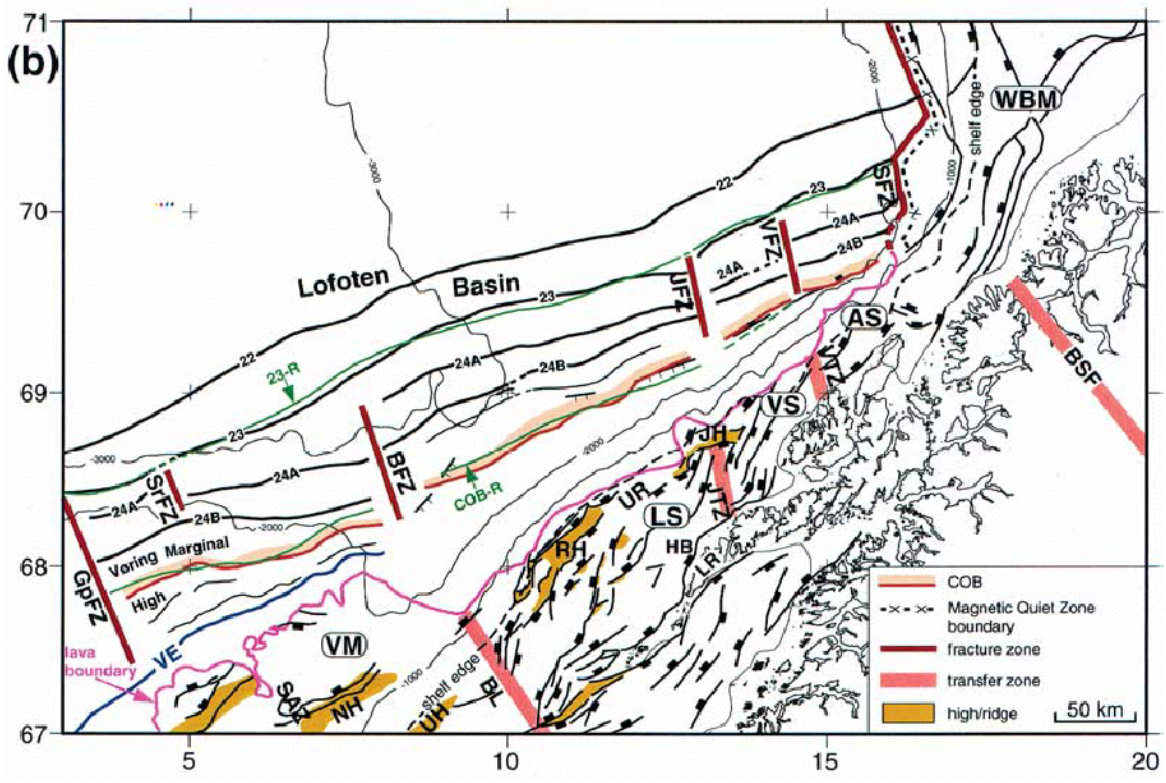

Figure 4.4 *Magnetic lineations and structural elements off Norway (Tsikalas et al. 2002). LS, VS, AS - Lofoten, Vesterålen, and Andøya margin segments, respectively; WBM – Western Barents Sea Margin; SA – Surt accommodation zone; NH, UH, RH, JH - Nyk, Utgard, Røst, and Jennegga highs, respectively; LR, UR - Lofoten and Utrøst ridges, respectively; HB, Havbåen sub-basin. GlFZ – Gleipne Fracture Zone; SrFZ – Surt Fracture Zone; BFZ – Bivrost Fracture Zone; JFZ – Jennegga fracture Zone; VFZ – Vesterålen Fracture Zone; SFZ – Senja Fracture Zone. 23-R and COB-R are conjugate features rotated from the Greenland margin.*

In the first RA-3 report it was mentioned that Berndt et al. (2001) interpreted the Lofoten lava flows to have been extruded in a submarine environment. However, the Vøring Escarpment (well expressed on magnetic data, see e.g. Fig. 2.4) has been proposed to mark a palaeo-coastline (e.g. Planke et al. 1999), along which the scarp formed by rapid chilling of the subaerial lavas as they reached the sea. Unless the Lofoten lava flows are of a different age than the Vøring lava flows, it is difficult to understand how the palaeo coastline could have ended at the northern tip of the Vøring Escarpment. If the Vøring Marginal High was above sea level and the Lofoten margin below sea level, the escarpment should swing to the west, marking the northern termination of a volcanic island or peninsula (the Vøring Marginal High and its E Greenland correlative). This is not the case. On the other hand, if the Lofoten lavas were extruded subaerially instead of being submarine, the palaeo-coastline should swing northeast from the Vøring Marginal High to the landward side of the Utrøst Ridge. Such a proposition appears just as difficult to support since the escarpment ends along a linear trajectory. Conceivably, the Vøring escarpment does not represent a palaeo-coastline, but instead marks a tectonic break that postdates the lava flows.

The sea-floor spreading magnetic anomalies 22-24B (Talwani & Eldholm 1977, Eldholm et al. 1979, Hagevang et al. 1983) are revealed in Figs. 2.1 & 2.4. Anomalies 24 A and 24 B refer to Chron 24n1n (52.51 Ma) and 24n3n (53.13 Ma), respectively (Cande & Kent 1995). Various NNW-SSE oriented oceanic fracture zones (Figs. 4.3 – 4.4) have previously been interpreted in the Nordland-Troms area: the Gleipne, Surt, Bivrost, Jennegga, Vesterålen and Senja fracture zones (Hagevang et al. 1983, Blystad et al. 1995, Tsikalas et al. 2001). Olesen et al. (2002, 2003) argued that the large variation in previous interpretations were partly due to the wide line spacing and low quality of navigation and levelling of the previous aeromagnetic surveys. Tsikalas et al. (2002) applied the aeromagnetic compilation of Verhoef et al. (1996) consisting of a 5 x 5 km grid. The grid cell size is consequently in the same order as the interpreted offsets. Tsikalas et al. (2002) correlated the "fracture zones" on the Vøring-Lofoten margin with similar apparent breaks in the spreading anomalies 24 A and B on the conjugate Greenland margin where the line spacing (10-20 km) is larger than for most areas along the Norwegian continental margin (4-15 km line spacing). Since the fracture zones on the Norwegian margin do not appear to be real features, but relate to data problems, we question the existence of the correlative NE Greenland fracture zones.

5. RESULTS

5.1 Oldest (innermost) seafloor anomalies along the Vøring-Lofoten and conjugate NE Greenland margins

Reconstruction of the NE Atlantic is somewhat complicated, mainly due to the Aegir and Kolbeinsey Ridge pair. This ridge pair is commonly interpreted to represent a ridge jump from the Aegir to Kolbeinsey Ridge (e.g. Talwani & Eldholm 1977), but the ridges have also been suggested to represent overlapping opposed spreading axes (e.g. Nunns 1983, Larsen 1988, Lundin & Doré in press). For the purpose of this report, it is convenient to subdivide the NE Atlantic into three segments: a) a southern Reykjanes Ridge segment, b) a central Aegir and Kolbeinsey Ridge segment, and c) a northern Mohns Ridge segment. Magnetic anomalies are comparatively straightforward to interpret along the Reykjanes and Mohns Ridges. We need not be concerned with the more complicated central segment, as long as one accepts the assumption of rigid plate behaviour (i.e. that the Greenland and Baltica cratons are not broken by major shears) and assuming that significant post-breakup deformation has not occurred.

Reconstructions of the oldest magnetic seafloor anomalies (Anomaly 24B to 23) along the Reykjanes and northern half of Mohns Ridges provide a good fit (e.g. Mosar et al., 2002). However, the same is not true for the southern Mohns Ridge where a gap occurs, i.e. between the SW Vøring and conjugate NE Greenland margins. Hagevang et al. (1983) proposed an abandoned spreading ridge on the Norwegian side of the southernmost Mohns Ridge (Figs. 4.3 & 4.4). Such a model naturally implies the lack of equivalent age seafloor off the conjugate NE

Greenland margin. Following the work by Hagevang et al. (1983) several workers (e.g. Escher & Pulvertaft 1995, Larsen 1990) continued to place the COB of the southern NE Greenland margin along a marked free air gravity anomaly. This COB interpretation results in a geometry where the oldest NE Greenland anomalies appear "truncated" southwards against the COB, i.e. they are shorter than younger anomalies. However, in more recent time it has become apparent that the oldest magnetic anomalies of the Mohns Ridge may continue underneath the NE Greenland shelf (e.g. Scott, 2000) (Figs. 5.1 & 5.2); the uncompensated Neogene shelf is responsible for the free air gravity anomaly previously interpreted as the COB. These southernmost magnetic anomalies are more diffuse, broader, and of higher amplitude than the narrower and more distinct linear seafloor anomalies along the northern Mohns Ridge. This diffuse and broad magnetic anomaly pattern also characterises the conjugate Norwegian margin (Figs. 2.1, 3.1 & 5.3).

The reconstruction gap along the southern Mohns Ridge probably reflects different origins to the northern and southern anomalies. Comparison with younger seafloor anomalies (Chron 22 and younger) suggests that the northern anomalies mark traditional seafloor, whereas the broad and diffuse southern anomalies may represent a mixture of seafloor and intruded continental crust. Such an interpretation is supported by the fact that the broad and diffuse magnetic anomalies along the SE Vøring margin coincide with a significant bathymetric high, the Vøring Plateau. As shown by Fig 5.1 (e.g. bathymetry with magnetic anomaly overlay), the oldest magnetic anomalies "climb" up the slope of the Vøring Plateau, which long has been suggested to represent an area of anomalous magmatism (e.g. Vink 1984).

It is conceivable that the Mohns Ridge was part of a linked, southward propagating ridge system (consisting of the Nansen, Mohns, and Aegir Ridges) (Fig. 5.4). If so, the Reykjanes and Kolbeisney Ridges formed an opposed northward-directed propagating ridge system. An empiric correlation appears to exist between the tips of the individual ridge segments and areas of increased magmatism. A reconstruction of the Mohns Ridge to Chron 22 (c. 49 - 49.7 Ma) indicates that the broad, diffuse, high amplitude magnetic anomalies on the Vøring margin may correlate with similar anomalies along the West Jan Mayen Fracture Zone (WJMFZ). Inboard of these anomalies in East Greenland lie several intrusive complexes. Age dating of these dominantly alkaline intrusions span between c. 24 and 47 Ma, but the wide age span probably reflects the mixture of K/Ar, Rb/Sr, and Ar/Ar age dating methods as well as a mixture of whole rock and separate mineral analyses (summarised in Torsvik et al. 2001, Nielsen 2002 and Lundin & Doré 2002).

Nielsen (1987) and Larsen (1988) referred to an initial magmatic lineament (IML) located between the Kangerlussuaq and Traill Ø region, i.e. along a "short cut" line connecting the proto-Mohns and Reykjanes Ridges. The IML may relate to a failed attempt of direct linkage between the Reykjanes and Mohns Ridges (Larsen 1988). Here we extend this idea further and speculate that the above-mentioned broad and diffuse magnetic anomalies along the Vøring margin and extending to the Traill Ø region may have developed as part of the IML (Fig. 5.5). While the various intrusions in East Greenland remain somewhat poorly dated, magmatic rocks in the Kangerlussuaq area are better constrained and are dominated by a c. 50 Ma event (e.g. Noble et al. 1988). This timing corresponds well with a possible Chron 22 event to the north.

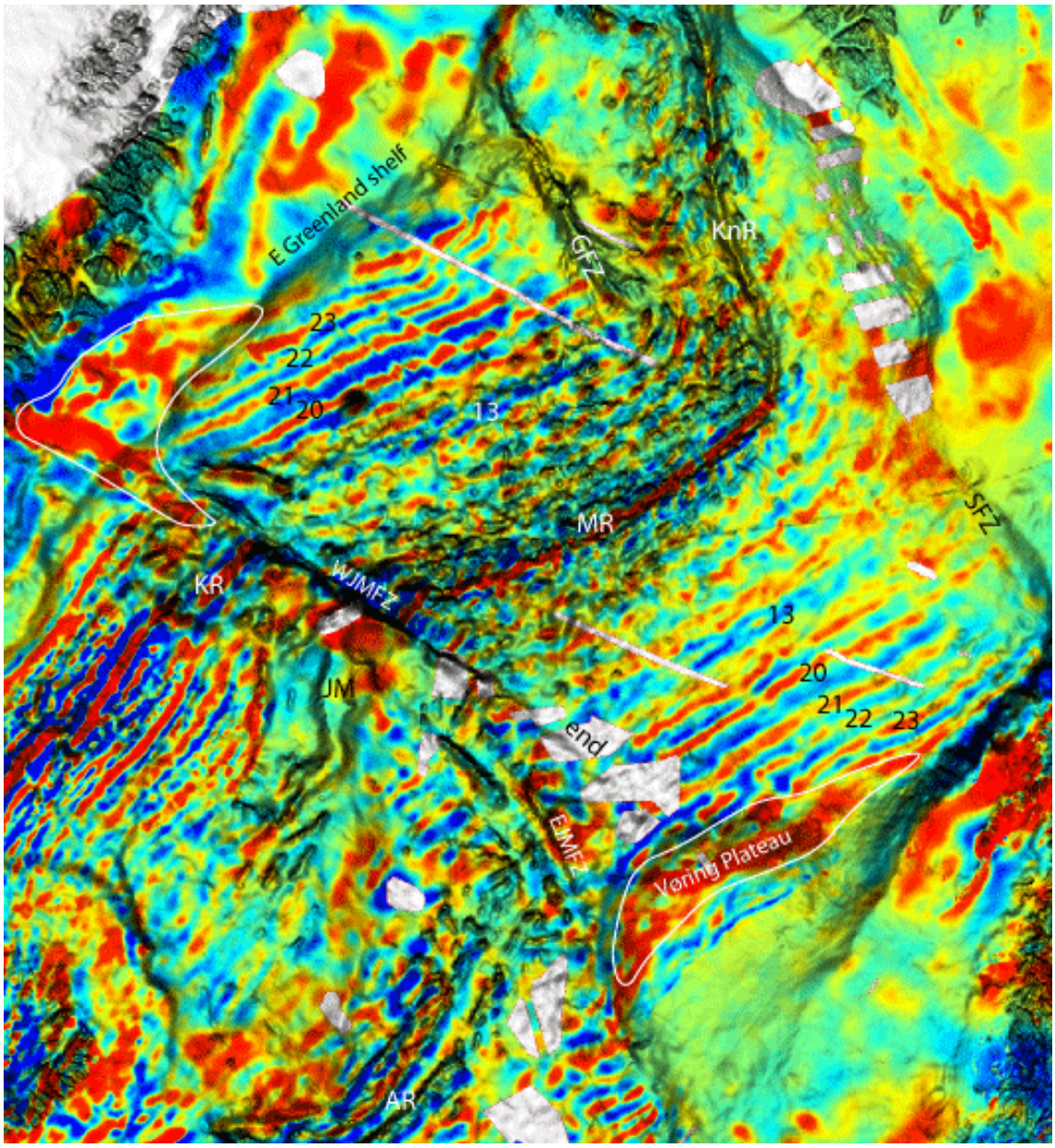

Figure 5.1 *Map view of total magnetic field draped on bathymetry/topography, illuminated from the south with an 80ºsun angle. Note the anomalous magnetic signature within areas outlined in white. The E Greenland shelf edge sets up a pronounced free air gravimetric anomaly, which in the past erroneously has been interpreted as the continent-ocean boundary (COB). Note that the oldest magnetic anomalies along the Mohns Ridges on the Norwegian side climb up the slope of the Vøring Plateau. See Fig. 5.2 for a perspective view. Abbreviations: AR - Aegir Ridge, EJMFZ - East Jan Mayen Fracture Zone, GFZ - Greenland Fracture Zone, JM - Jan Mayen microcontinent, MR = Mohns Ridge, KR - Kolbeisney Ridge, KnR - Knipovich Ridge. SFZ - Senja Fracture Zone, WJMFZ - West Jan Mayen Fracture Zone, 'end' – eastern termination of WJMFZ. Numbers refer to magnetic chrons.*

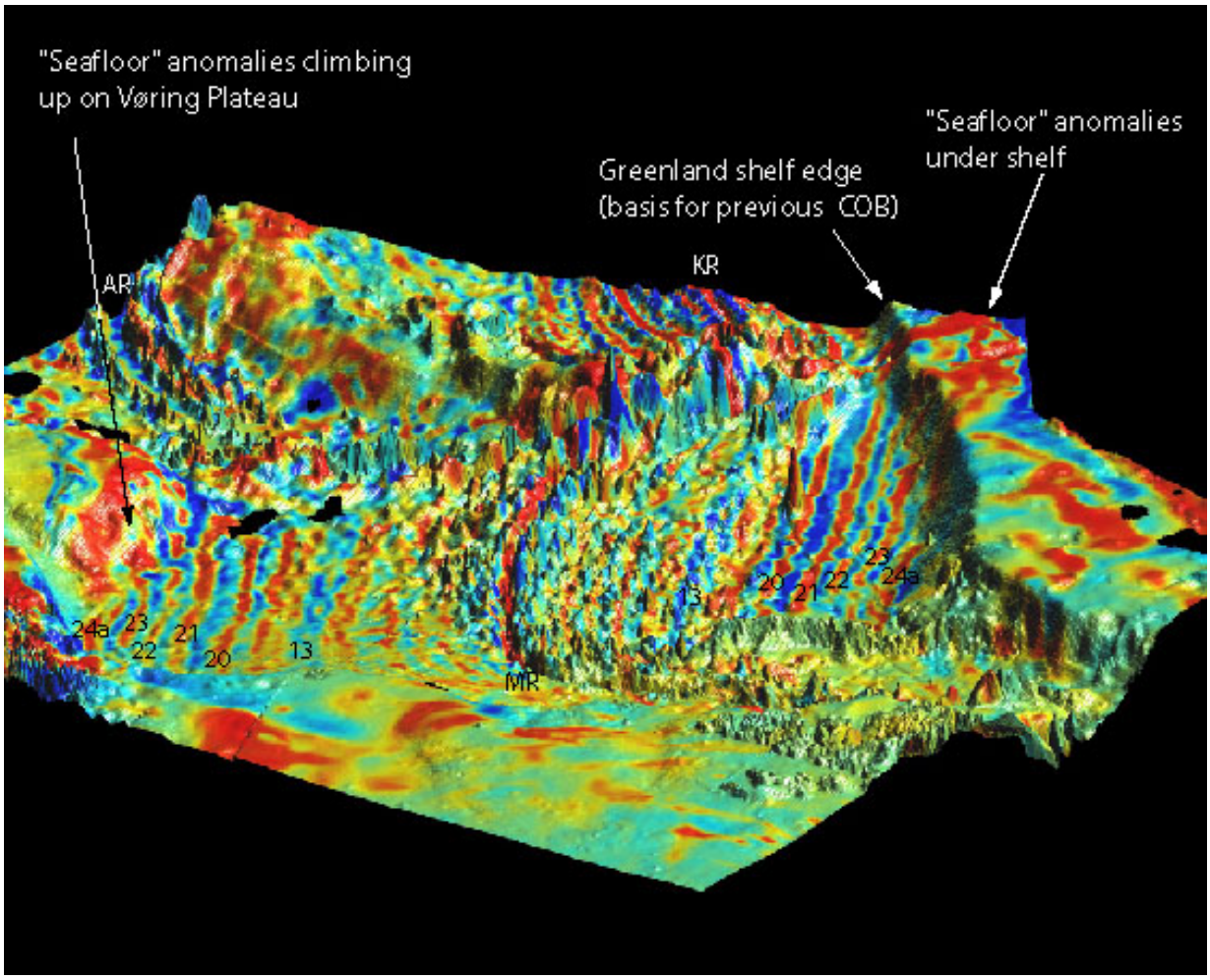

Figure 5.2 Perspective view of Fig. 5.1 from the north. Note how the oldest magnetic anomalies climb up on the slope of the Vøring Plateau. Abbreviations as in Fig. 5.1.

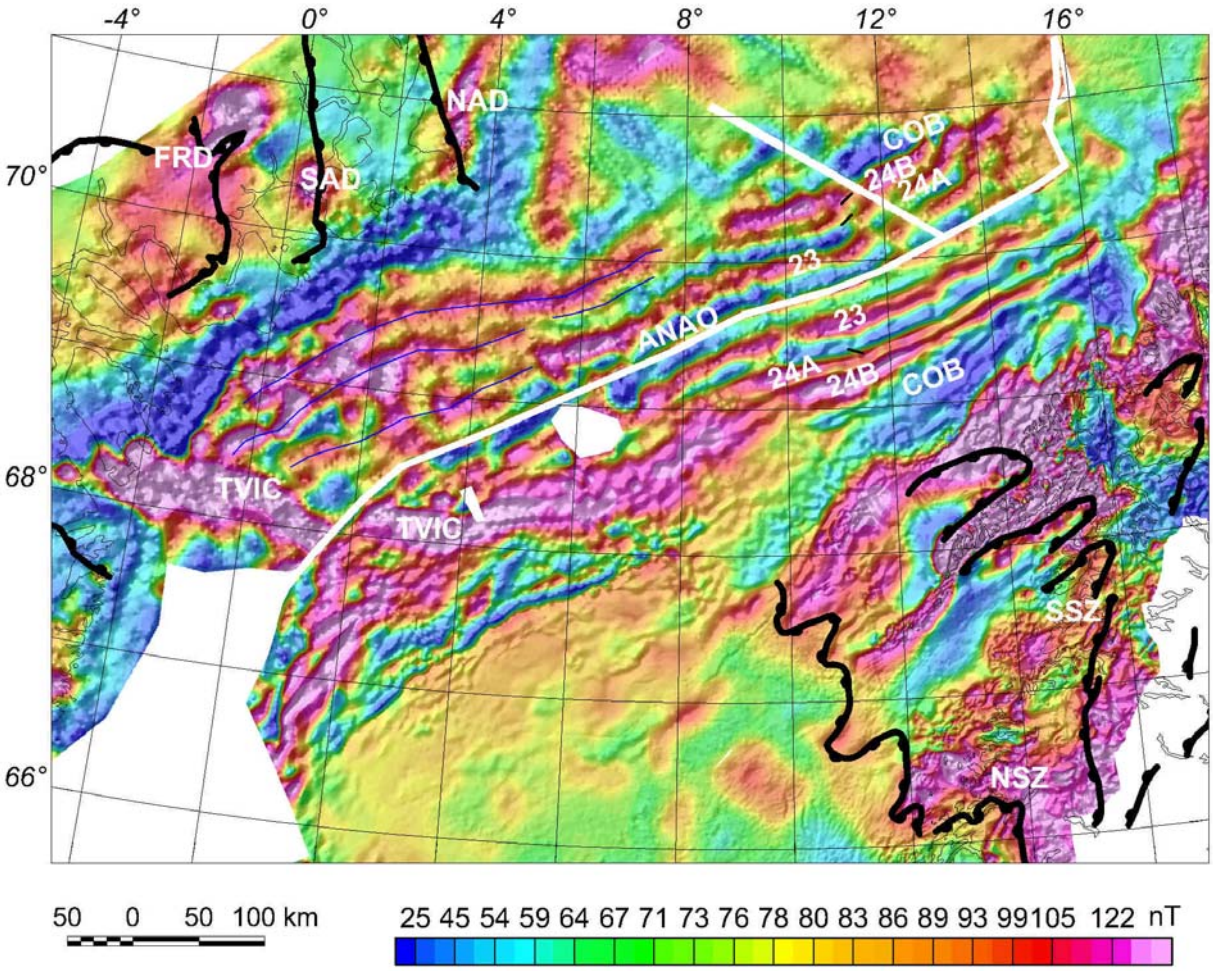

Figure 5.3 Reconstruction of the Greenland margin aeromagnetic data to Chron 22 (c. 49.7 Ma). Note that the c. 50 km wide, diffuse, high amplitude aeromagnetic anomaly to the NW of the Vøring Marginal High appears to be continuous across the oceanic spreading anomalies 23, 24A and 24B as far as to Traill Ø (on the east Greenland coast) where Tertiary igneous complexes occur at the surface. This anomaly has earlier been interpreted as anomalies 24A and 24B in the Norwegian Sea. The width of the anomaly is, however, considerably wider than the corresponding anomalies offshore Lofoten further to the north. The anomaly is most likely caused by an igneous complex (refereed to as Traill Ø-Vøring igneous complex in the present report). The introduction of this igneous complex simplifies the initial opening history and excludes the need to invoke the abandoned spreading ridge and the Gleipne Fracture Zone along the Vøring margin.

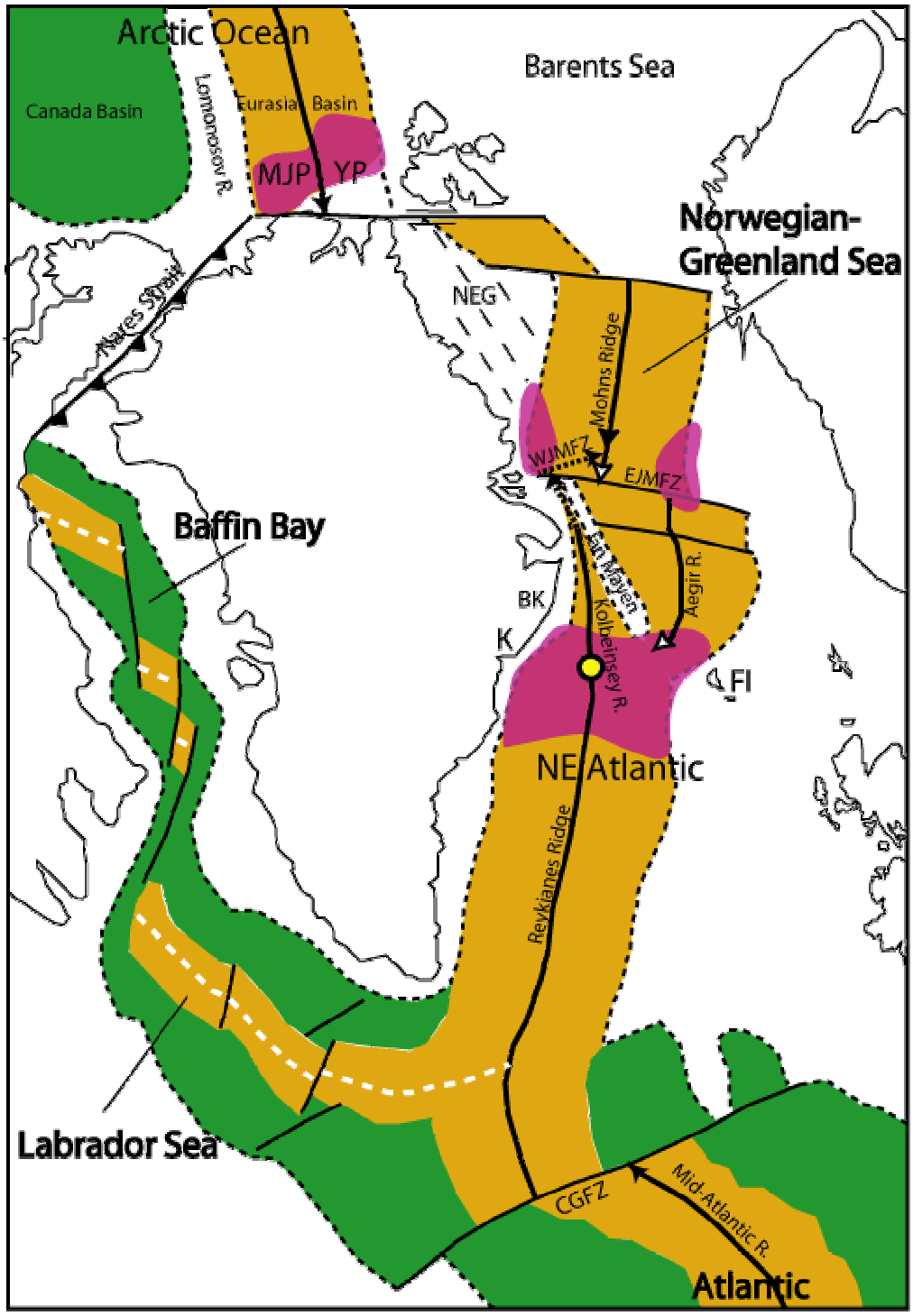

Figure 5.4 *Simplified reconstruction to Chron 13 (c. 33.3 Ma), illustrating a conceptual model for opposed and overlapping spreading ridges. The Arctic system consisted of the Nansen, Mohns, and Aegir Ridges, while the North Atlantic system consisted of the Reykjanes and Kolbeisney Ridges. Areas of pronounced magmatism outlined in purple. NEG – Northeastern Greenland shelf; MJP – Morris-Jesup Plateau; YP – Yermak Plateau; WJMFZ – Western Jan Mayen Fracture Zone; EJMFZ – Eastern Jan Mayen Fracture Zone; BK- Blossville Kyst; K – Kangerlussuaq; FI – Faeoe Island; CGFZ – Charlie Gibbs Fracture Zone The yellow dot represents the Iceland plume centre. From Lundin et al. (2002).*

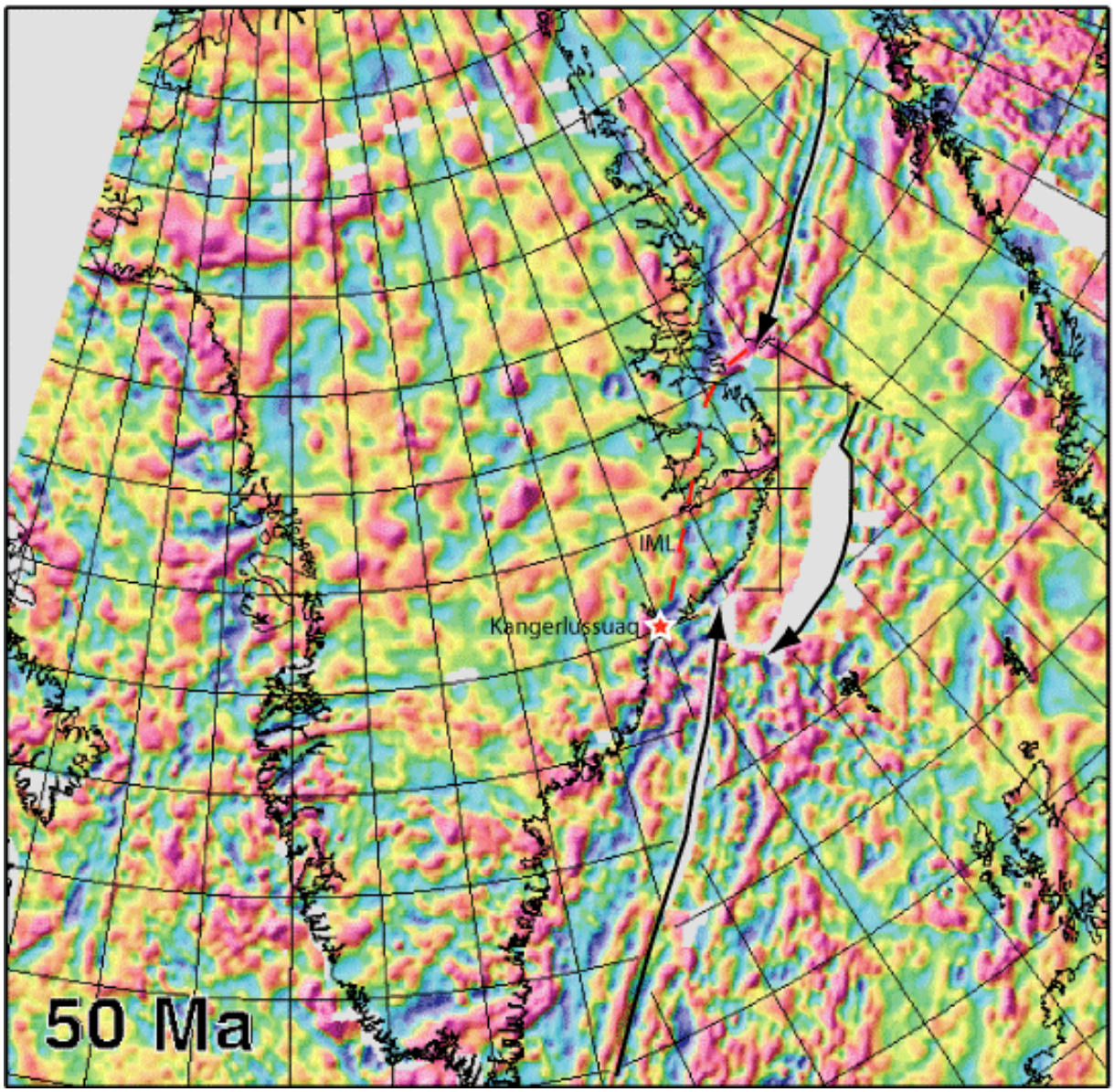

Figure 5.5 *Reconstruction of the NE Atlantic magnetic data to 50 Ma. Note that this reconstruction only addresses the NE Atlantic, not the Labrador Sea (Lundin et al., 2002). IML - initial magmatic lineament (IML) located between the Kangerlussuaq and Traill Ø region, i.e. along a "short cut" line connecting the proto-Mohns and Reykjanes Ridges.*

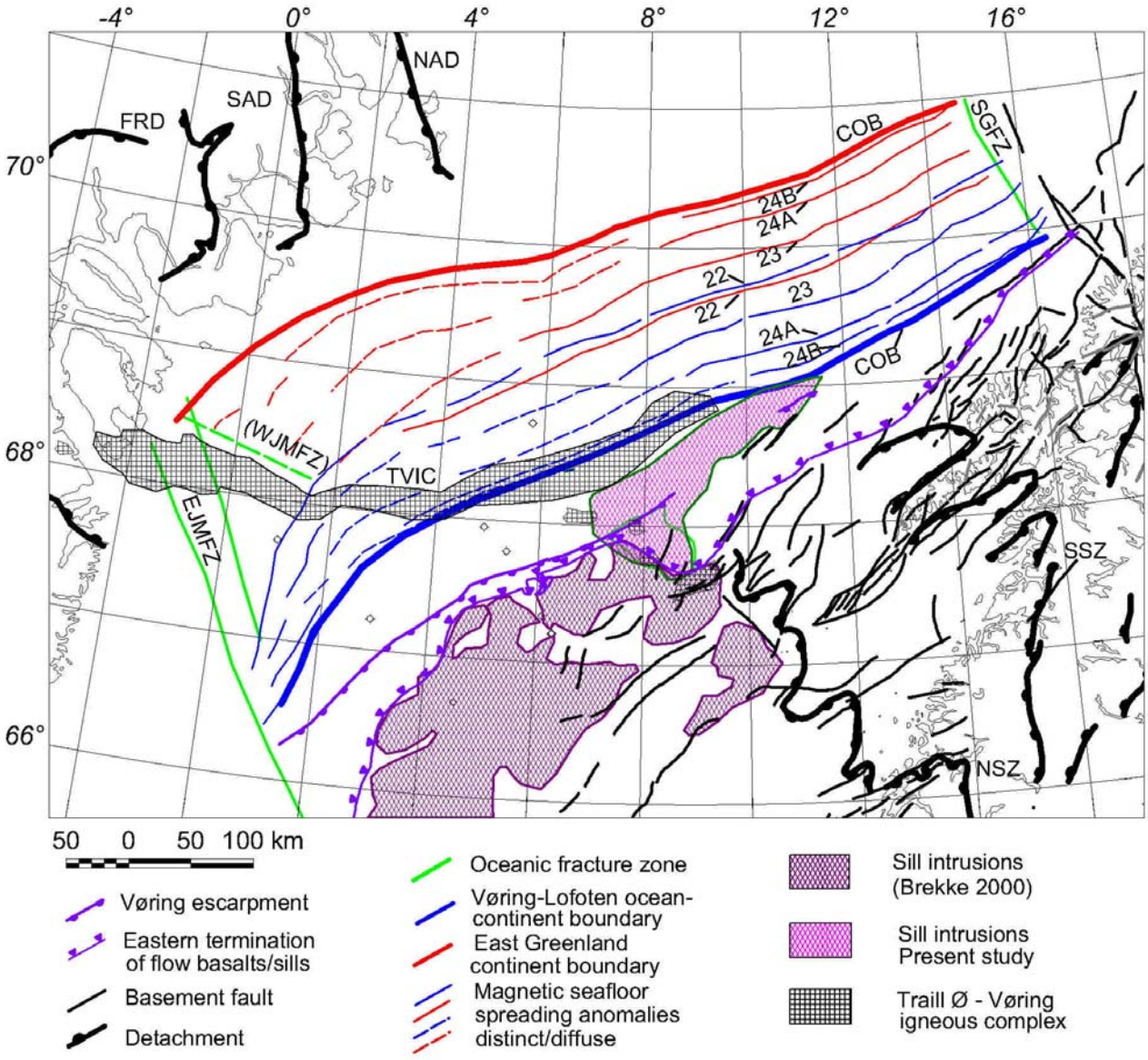

Figure 5.6 *Reconstruction to Chron 22 (49.7 Ma). Regional basement faults and sill intrusions on the Vøring-Lofoten continental margin. COB – continent-ocean boundary; EJMFZ – Eastern Jan Mayen Fracture Zone; (WJMFZ) – future location of Western Jan Mayen Fracture Zone; TVIC – Traill Ø – Vøring igneous complex; SSZ – Sagfjord Shear Zone; NSZ – Nesna Shear Zone; NAD – Northern Ardencaple Fjord Detachment; SAD – Southern Ardencaple Fjord Detachment; FRD – Fjord Region Detachment system.*

5.2 3D model of the Surt Lineament

The presented model is an enhancement of the model presented in Part 1 of the Ra 3 interpretation report. The new model was created to mainly study two topics in more detail:

- Tectonic relevance of the Surt Lineament

The Surt Lineament is located in the south of the model presented in Part 1 of the Ra3 report. Because of its position near the edge of the original model we were not able to evaluate its tectonic role. Conceivably, the Surt Lineament might be the offshore continuation of the Kollstraumen detachment, which is the northern boundary of the Central Norway basement window. Our extended model allows detection of structural changes, if present, along the offshore continuation if this structure. Hence, this modelling is able to test the possibility that the Surt Lineament is an offshore continuation of the Kollstraumen detachment.

-Identification of magnetic sources south of the Bivrost Lineament

The model presented in Part 1 of the Ra 3 Report was not adjusted to the magnetic anomalies in the southern study area, due to their relatively small amplitudes. However, comparison to the solutions of Euler deconvolution and introduction of highly magnetic sills can improve the model.

The model now consists of 16 parallel cross-sections in the study area with a distance of 20-35 km (see Fig. 5.7-5.10).

We present the cross-sections L12, L13, L14, L14.5 and L15 (Figs. 5.11 - 5.15). These are the cross-sections, which are new or to which changes have been applied. In addition we also present a cross-section (Fig. 5.16) in SW-NE direction through the 3D model, located close to two OBS lines (Line 3 of Mjelde et al. 1997 and Line 7 of Mjelde et al. 1998). All new profiles are located within the OBS networks presented by Mjelde et al. (1997, 1998, 2001, 2003a,b,c).

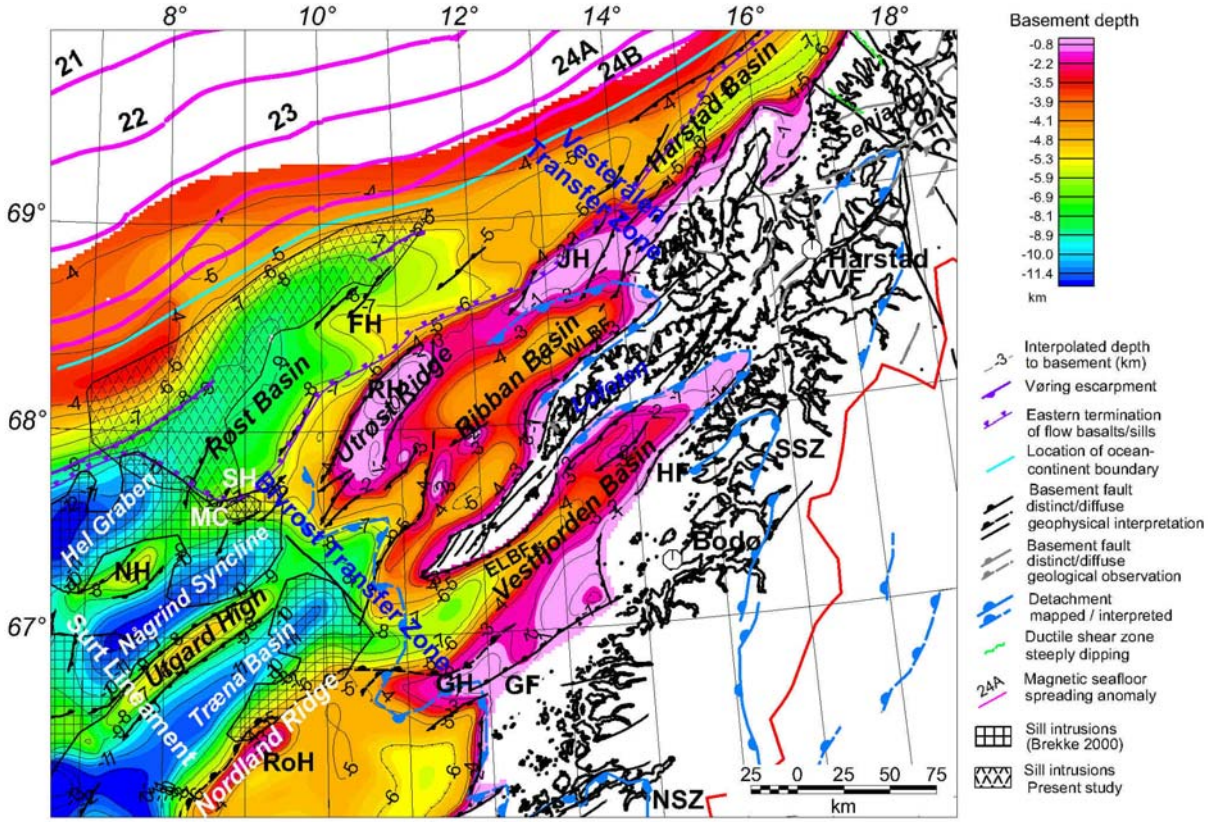

Figure 5.7 *Regional basement structures within the Nordland area. The depth to basement surface represents depth to crystalline rocks. NSZ - Nesna shear zone, SSZ - Sagfjord shear zone; GF - Grønna fault, HF - Hamarøya fault; FH - Flakstad High; J – Jennegga High; SH – Sandflesa High; RH – Røst High; NH – Nyk High; RoH – Rødøy High; GH – Grønøy High; VFZ – Vesterdjupet Fault Zone; BSFC – Bothnian-Senja fault complex; VVF – Vestfjorden-Vanna fault complex; WLBF – Western Lofoten border fault; ELBF – Eastern Lofoten border fault; MC – Myken volcanic complex. The nomenclature is adapted from Andresen & Forslund (1987), Blystad et al. (1995), Løseth & Tveten (1996), Olesen et al. (1997, 2002, 2003,) Tsikalas et al. (2001) and Braathen et al. (2002).*

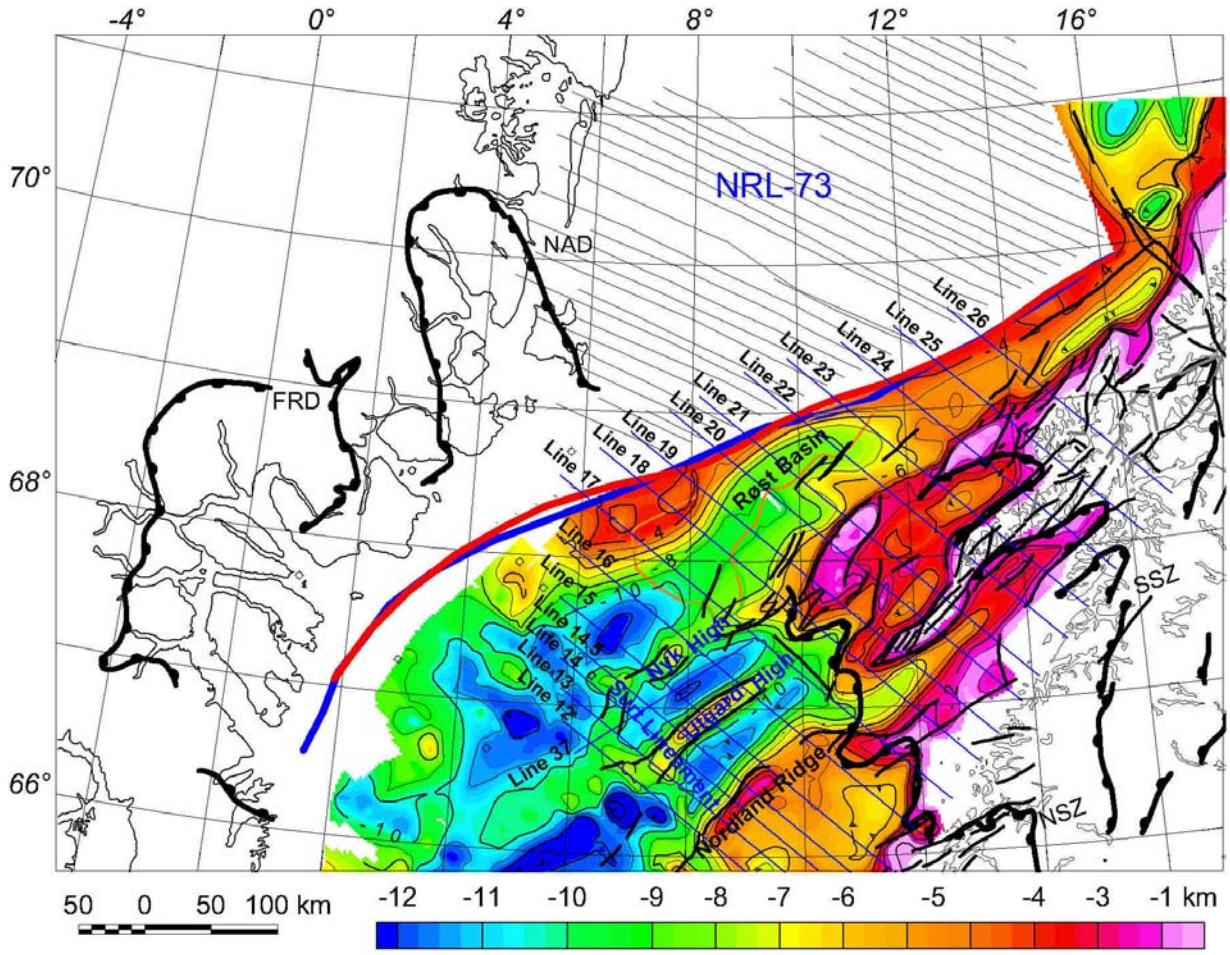

Figure 5.8 *Reconstruction to the Eocene opening of the North Atlantic. Regional basement faults on the Vøring-Lofoten continental margin. Interpretation of depth to crystalline basement, modified from Olesen et al. (2002, 2003). The bold black lines show late Caledonian detachment zones (Hartz et al. 2002, Braathen et al. 2002, Olesen et al. 2002). SSZ – Sagfjord Shear Zone; NSZ – Nesna Shear Zone; NAD – Northern Ardencaple Fjord Detachment; SAD – Southern Ardencaple Fjord Detachment; FRD – Fjord Region Detachment system. NRL-73 – Naval Research Laboratory 1973 aeromagnetic survey.*

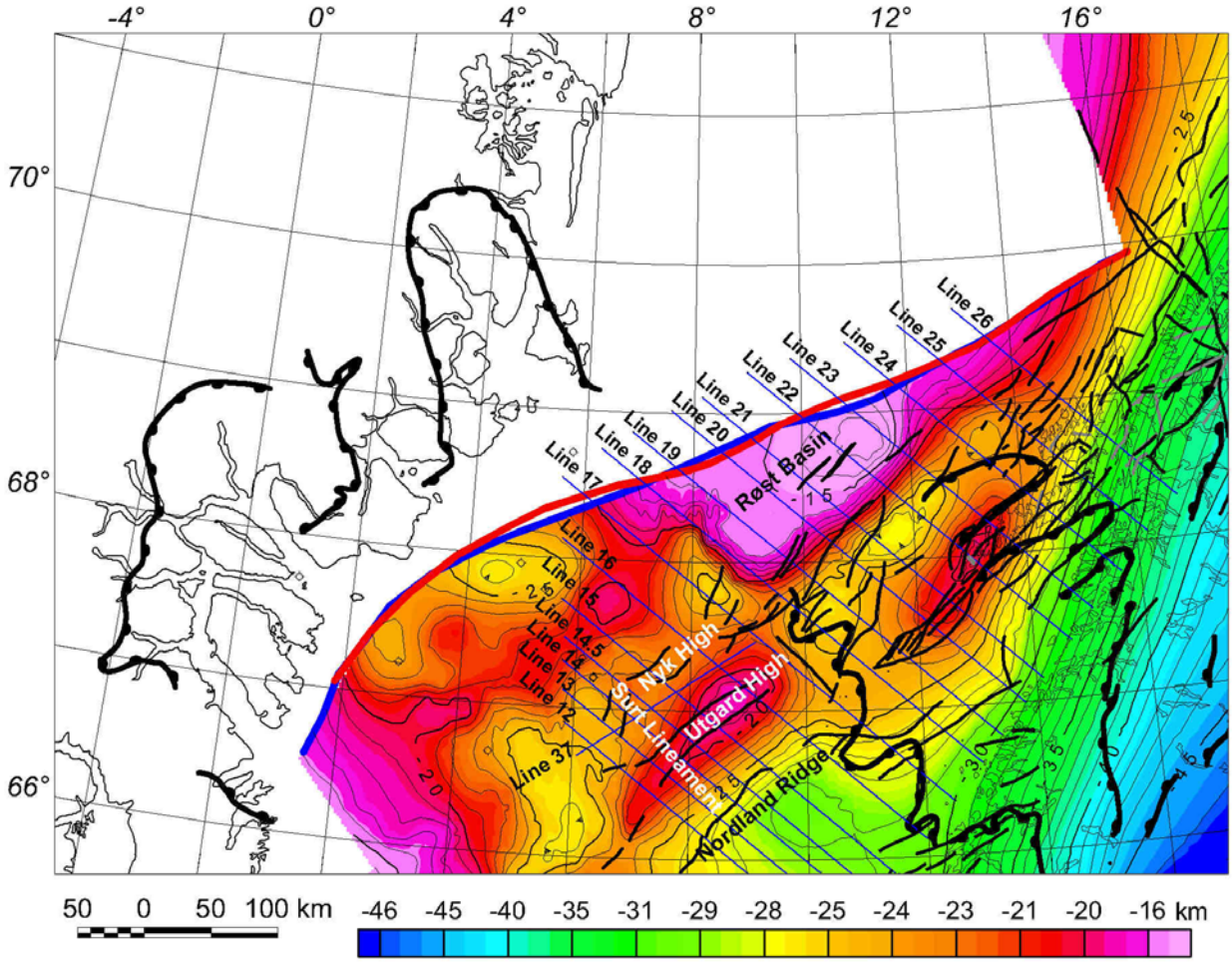

Figure 5.9 Reconstruction to the Eocene opening of the North Atlantic. Depth to Moho compiled from refraction seismic studies (Lund 1979, Kinck et al. 1993, Mjelde et al. 1992, 1993, 1997, 1998, Sellevoll 1983) and gravity interpretations (Olesen et al. 1997, 2002). The thin blue lines show the interpreted profiles within the 3D model. The bold blue line denotes the interpreted continent-ocean boundary (COB) on the Norwegian margin while the red line shows the rotated COB on the Greenland margin. The bold black lines show late Caledonian detachment zones (Rykkelid & Andresen 1994, Hartz et al. 2002, Braathen et al. 2002, Olesen et al. 2002, Steltenpohl 2004).

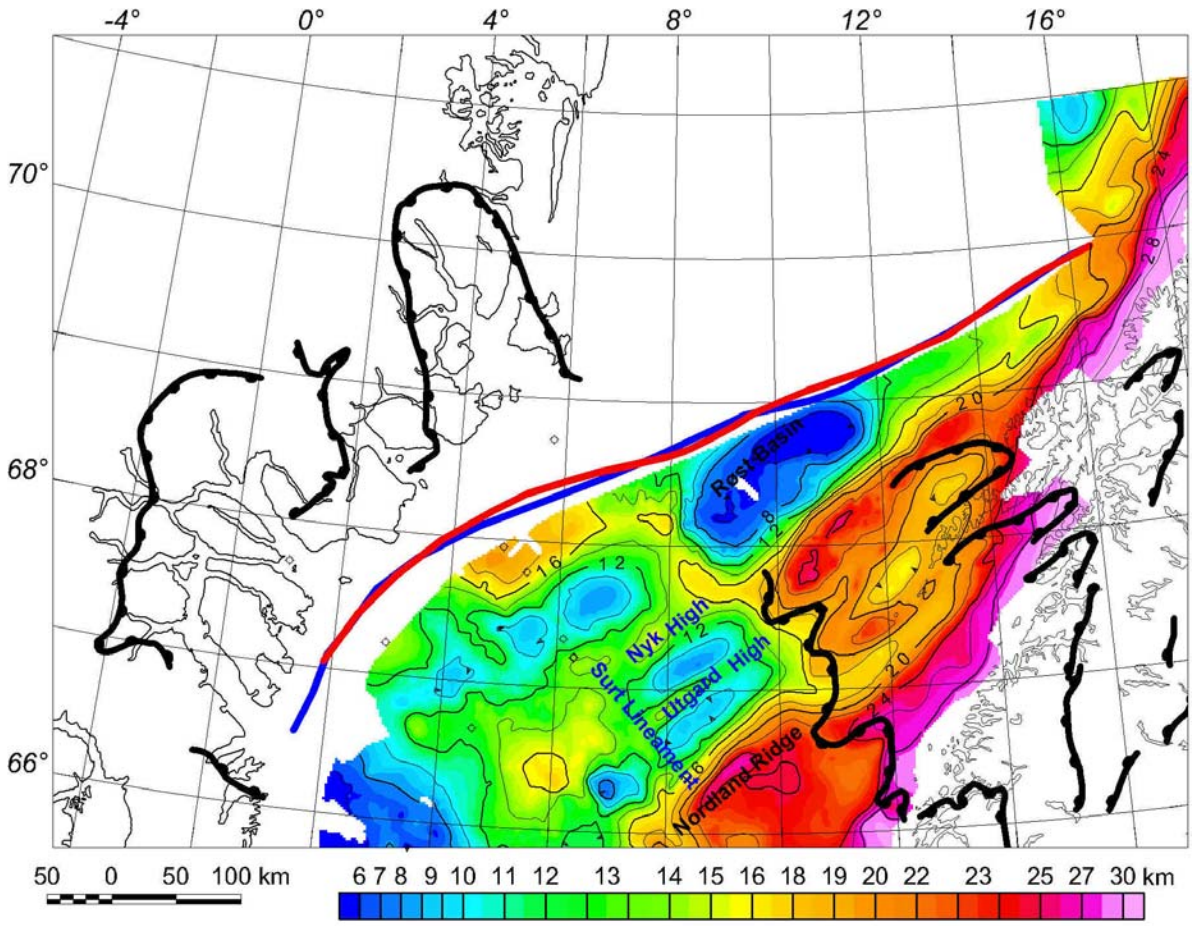

Figure 5.10 *Thickness of the crystalline basement obtained by subtracting the depth to basement (Fig. 5.8) from the depth to Moho (Fig. 5.9). Note that the lower crustal high velocity body underneath the Vøring margin is included in the basement thickness. The basement thickness in the Vøring area is relatively uniform compared to the to the Lofoten region where the shelf area has a significantly thicker basement than the Røst Basin to the NW. The average basement thickness across the Vøring and Lofoten margin sectors may, however, be relatively uniform.*

5.2.1 3D gravity model

The two most important parameters for constructing the 3D density model are the geometry and the density of the structures. The densities used in the model process are based on published values (Mjelde et al. 1998, Olesen et al. 2002, Olesen and Smethurst 1995, Olesen and Torsvik 1993). The densities in these studies are based on different sources as velocity-density relationships (e.g. Ludwig et al. 1970). The values in the present study are consistent with previous work. In addition to the density structure of the crust (as described below), the lithospheric mantle was modelled by assuming a stepwise increase (200 K) in temperature from the Moho (c. 500°C) to the asthenosphere at a temperature of c. 1300 °C (see Part 1 for further details).

To constrain the geometry of the model, a variety of geological and seismic investigations have been considered. The main control on the regional structure of the area surrounding the Surt Lineament is gained by the results of an OBS network (Mjelde et al. 1997, 1998, 2001, 2003 a, b, c). Additional information is among others given by the studies of Gernignon et al. (2002, 2003), Doré et al. (1999), Skogseid et al. (1992). Further seismic information is available along reflection profiles (Ebbing 2004).

The adjustment of the modelled gravity to the observed gravity anomalies is generally good. Only minor misfits occur, which can be explained by the limited resolution of the model. We will only describe the structures south of the Bivrost Lineament as we have not applied changes to the structures north of it, presented in Part 1 of the report.

5.2.2 Moho geometry and magmatic underplating

All the cross sections (Lines 12-17) south of the Bivrost Lineament feature a high-density lower crustal body (HDLC) at depth (Figs. 5.11-5.15). In the previous RA-3 report this lower crustal body was referred to as magmatic underplated material, but in order to avoid a genetic connotation we simply refer to the HDLC. The existence of this HDLC is constrained by OBS studies (in these data defined as a high-velocity body) in the northern and central Vøring Basin (e.g. Mjelde et al. 1998). The HDLC may have been emplaced as thick magmatic intrusions into the lower crust on both sides of the Vøring escarpment during the break-up and seafloor spreading between Eurasia and Greenland (Eldholm & Grue 1994, Skogseid et al. 1992). The south-western boundary of the HDLC coincides with a shallow Moho below the Utgard High and on the southern profiles below the Fles Fault Complex.

The cross line also reveals that the HDLC thins to the north-east, disappearing north of the Bivrost Lineament. We have shown in Part 1 that there is no HDLC present north of the Bivrost Lineament.

5.2.3 Crustal density

In comparison to the results presented in the Ra 3 Report, Part 1, the density of the upper part of the crust is 2800 kg/m^3 (compared to 2850 kg/m^3 previously). This change has been applied to give a better adjustment to the anomalies, but lies within the range of uncertainties from velocity-density-conversions. The main part of the upper crust still has a density of 2850 kg/m^3. The density of the lower crust east of the Utgard High/Fles Fault Complex is 2950 kg/m^3, but to the west and above the HDLC, the density had to be increased to 3000 kg/m^3. This can be explained by the presence of sills/volcanic material with higher density.

5.2.4 Depth to basement

The crustal densities and the geometry of the Moho are mainly causing the long wavelength changes in the gravity field. The geometry of the sedimentary basins and the basement depth also affect the long-wavelength anomalies, but adds additional medium- to short-wavelength components.

The geometry of the sedimentary basins correlates with the gravity anomalies and reflect intrabasin features such as the Hel Graben, Nyk High, Någrind Syncline, Utgard High, and Træna Basin. All these structures are well detectable in the basement depth, while there is no significant change related to the Surt Lineament (see Fig. 5.16). Modelling of the density structure shows no signs of a structural change or a tectonic boundary connected to the Surt Lineament. To further evaluate this, the magnetic properties of the area have been studied in more detail.

5.2.5 3D magnetic structure

The 3D structure of the density model was interpreted to adjust the magnetic model within the surrounding of the Surt Lineament. The fit of the modelled magnetic anomaly to the observed anomaly is not as good as for the gravity field. The main focus was on modelling the gradient of the magnetic field, but not to model the amplitudes perfectly. Due to the dependency on the distance to the source masses, a better fit of the magnetic anomalies can only be achieved by a more detailed 3D model, which provides a higher resolution.

To partly overcome this shortcoming, the distance between the profile sections is reduced compared to the model presented in the Ra 3 Project Report Part 1. This helps to further identify the magnetic sources, which is especially important in the area, where the amplitudes of the magnetic anomalies vary between -150 and +100 nT.

5.2.6 Curie temperature

The magnetic data will only reveal information on the part of the model, which has a present temperature below the Curie temperature. Rocks at higher temperatures will not show the ferromagnetic behaviour necessary to generate the discernible magnetic signal. The dominant material is regarded to be magnetite, which has a Curie temperature of 580 ºC (cf. Hunt et al. 1995). This is the maximum Curie temperature of the rocks at depth. Basalt may for instance have a significantly lower Curie temperature, i.e. 300-350 ºC. Magnetic rocks within the crystalline basement usually have coarse-grained magnetite and consequently a higher effective Curie temperature.

The depth to the Curie temperature is estimated to be maximum 12.5 km at the ocean-continent transition, and linearly deepening landwards. Below the coastline a depth of 27.5 km was applied, which is 5 km deeper than for the model presented in Part 1. These new values would be corresponding to a constant temperature gradient from the surface to the Curie depth of 45 ºC/km at the continent/ocean boundary and 21 ºC/km at the coastline. These values are in the range of typical values for the continental shelf and oceanic crust. The estimate on the depth of the Curie-temperature is consistent with previous studies from the Lofoten area and the Vøring Basin (Fichler et al. 1999).

The deeper Curie temperature level below the coastline than in Part 1 is still in agreement with previous studies from the Vøring Basin (Fichler et al. 1999) and allows a better correlation of the regional magnetic trend between the modelled and observed magnetic field.

Comparison between the Curie temperature depth and the model shows that the boundary between magnetic and non-magnetic material generally runs through the lower continental and oceanic crust.

Magnetic sources

The amplitudes of the magnetic field south of the Bivrost Lineament are not as high as to the north and generally lie between -150 and 100 nT.

The model shows that the main sources of magnetic anomalies are related to

- the boundary between high and low magnetic basement (intrabasement contrasts)
- the depth of the sedimentary basins (suprabasement contrasts)
- the presence of intrusions

5.2.7 Basement and basins

The main magnetic material is expected to be in the basement, while the overlying sediments only have a small magnetic signature (e.g. susceptibilities in the order of 0.0003, Mørk et al. 2002). The susceptibilities of the basement can range between 0.003 and 0.01 (with Königsberg ratios between 0.3 and 1, Olesen et al. 2002, 2003).

The magnetic signature is therefore partly caused by the changing geometry between the low and the high magnetic basement. The inclination and declination of all remanent fields is set to 77.0º and 0.0º, approximately parallel to the present magnetic field, when not mentioned otherwise.

Figs. 5.11 – 5.15 show the cross-sections south of the Bivrost Lineament. The upper part of the basement has low susceptibilities (0.0025), while the lower basement has a higher value (0.0075). The modelling shows that the transition between high and low magnetic materials occurs in general at a depth of around 12 ± 2 km. The boundary between high and low magnetic basement shows small undulations, which mostly correlates with the depths to basement. In general, only the lowermost part of the basement can have high susceptibilities.

5.2.8 Comparison to Euler deconvolution

The solutions of the Euler deconvolution presented in Part 1 of the Ra3 interpretation report (Ch. 3.2) are projected on the cross-sections through the 3D model. The projection distance was 500 m and the points generally correlate well with the density/magnetic structure of the model. Only small changes had to be made to the original model of Part 1 to improve the correlations of the two methods. This is an indication of the high quality of the model and the Euler solutions.

The correlation shows again that the susceptibility contrast between the sedimentary basins and the basement and the transition from low magnetic to high magnetic basement are the main sources for the magnetic anomalies. E.g. on line 14 (Fig. 5.13) the solutions of Euler deconvolution coincide at the Utgard High with the top basement, while below the Træna Basins and Nordland Ridge the solutions are located at the low-high-magnetic basement transition.

5.2.9 Sills

In addition to the changes of susceptibilities from basements to sedimentary rocks and within the basement, the presence of sills has to be considered in the western part of the model. In the areas where the HDLC is interpreted there is also evidence for highly magnetic intrusions within the basins (Mjelde et al. 1997, 1998, Gernignon et al. 2003). The influence on the gravity field can be neglected as the volume of the sills is not very large and their effect on the gravity signature is masked by the shape of the sedimentary basins and the related uncertainties of sedimentary/crustal densities. However, these sills are supposed to be highly magnetic with both reversed and normal oriented magnetisation (see Table 2.6 I the Ra Project report Part 1, Olesen et al. (2003)) and have to be included to produce the observed magnetic anomalies in the western part of the study area.

5.2.10 Conclusions

The crustal structure across the Surt Lineament is demonstrated by the cross-section perpendicular to the Surt Lineament (Fig. 5.16). The geophysical parameters (density/susceptibility/Q-ratio) of the crust are similar on both sides of the Surt Lineament. There are minor changes within sedimentary densities, but these can be explained by the fact that the sedimentary basins to the south of the Surt Lineament are generally deeper than to the north. A deeper basin leads to more compaction of the sedimentary material with depth, which further increases in density. The differences are also relatively small with an average of 2500 kg/m^3 to the south, and 2450 kg/m^3 to the north of the Surt Lineament, which is in the range of uncertainty in density estimations. The same observations can be made for the magnetic structure. Here, the only new features are the sills located above the HDLC. We can, therefore, conclude that the Surt Lineament is not a regional tectonic boundary of the same importance as the Bivrost Lineament. The Surt Lineament is located in an area characterized by certain variations in basin depth, but does not separate basement rocks of different physical properties.

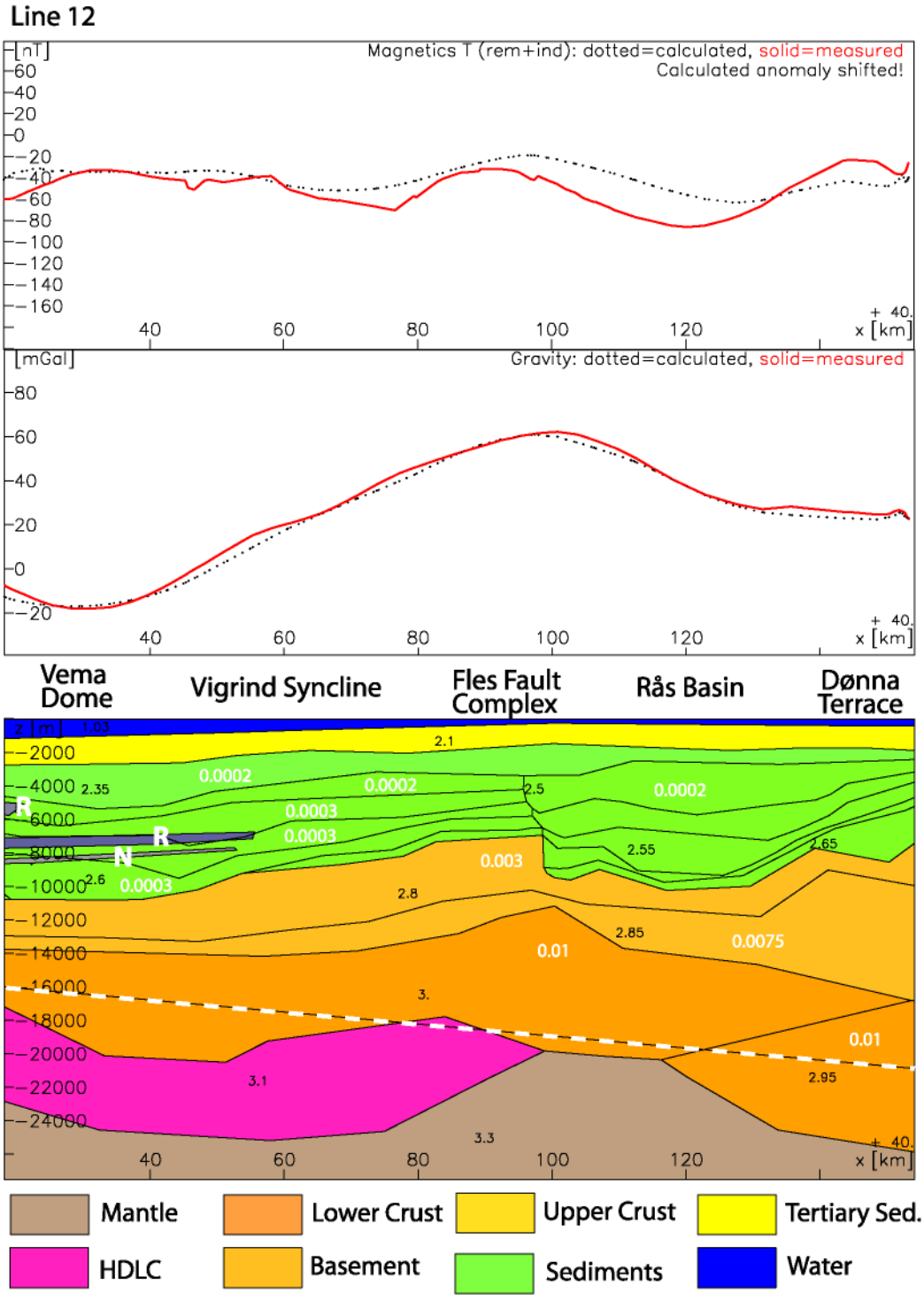

Figure 5.11 *Profile 12 of the 3D model. The upper panel shows the magnetic anomaly, the middle panel the gravity anomaly (offshore: Free-air anomaly, onshore: Bouguer anomaly) and the lower panel the modelled density/magnetic cross-section. The grey layers indicate sills with reversed (R) or normal (N) magnetisation. Black numbers are density values in 10^3 kg/m^3, white numbers represent magnetic susceptibilities. The black-white dotted line indicates the Curie depth. See Figs. 2.3 – 2.5, 5.8 & 5.9 for exact location of the section and text for further details.*

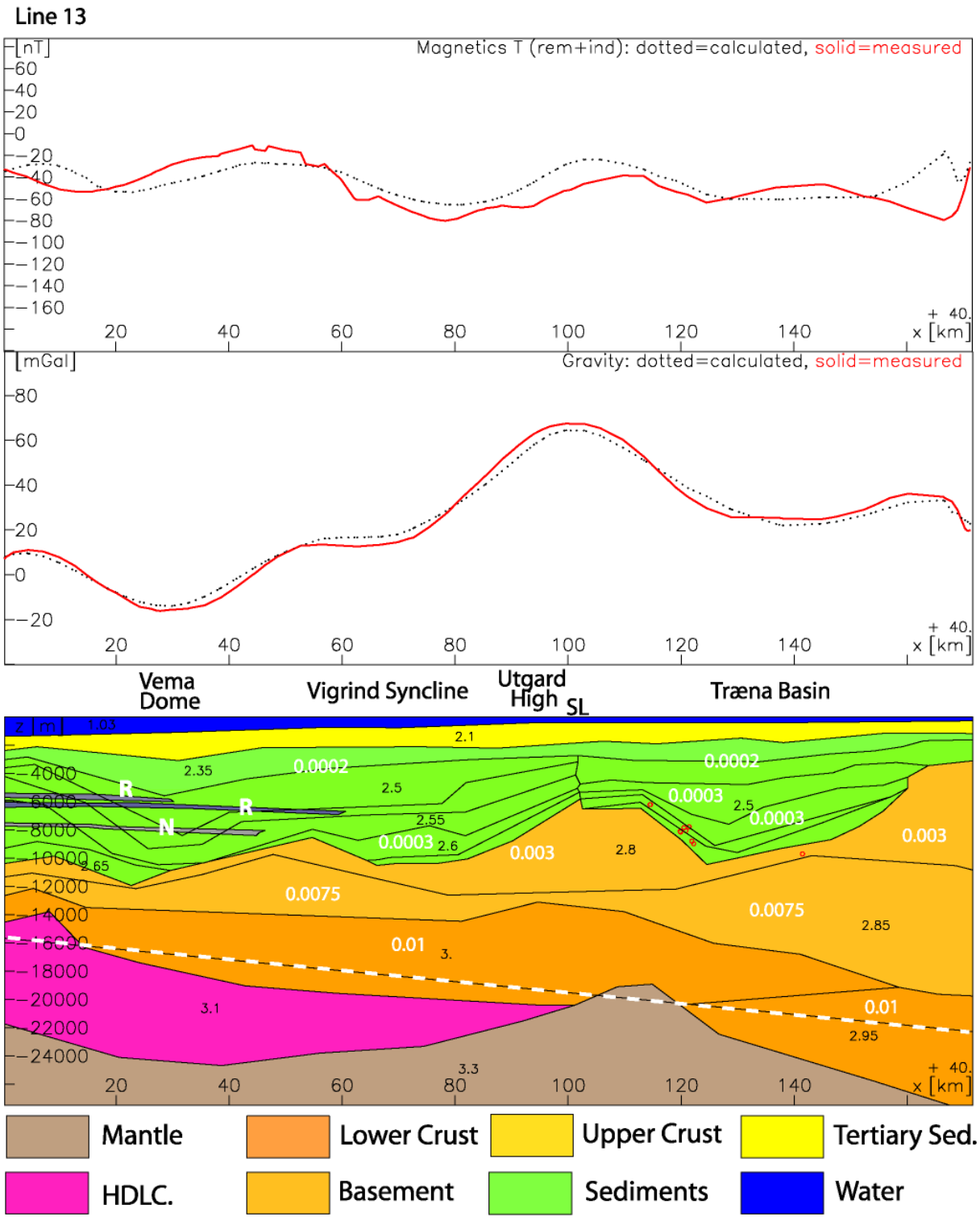

Figure 5.12 *Profile 13 of the 3D model. The upper panel shows the magnetic anomaly, the middle panel the gravity anomaly (offshore: Free-air anomaly, onshore: Bouguer anomaly) and the lower panel the modelled density/magnetic cross-section. The grey layers indicate sills with reversed (R) or normal (N) magnetisation. Black numbers are density values in 10^3 kg/m^3, white numbers represent magnetic susceptibilities. The black-white dotted line indicates the Curie depth. The red dots mark magnetic sources as calculated by Euler-deconvolution (see Chapter 3.2 of the Ra3 Project report Part 1 for details of analysis). SL indicates the location of the Surt Lineament. See Figs. 2.3 – 2.5, 5.8 & 5.9 for exact location of the section and text for further details.*

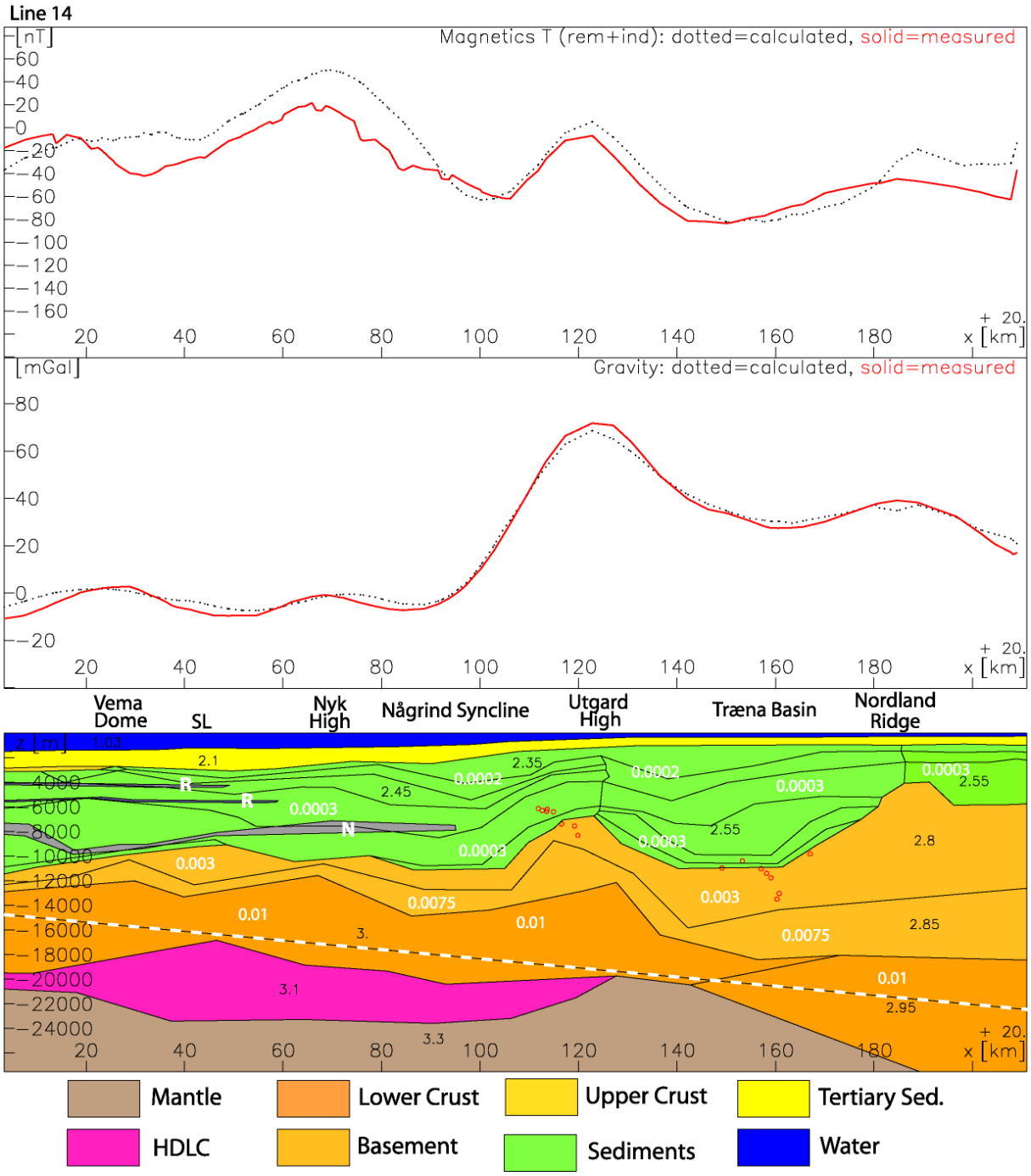

Figure 5.13 *Profile 14 of the 3D model. The upper panel shows the magnetic anomaly, the middle panel the gravity anomaly (offshore: Free-air anomaly, onshore: Bouguer anomaly) and the lower panel the modelled density/magnetic cross-section. The grey layers indicate sills with reversed (R) or normal (N) magnetisation. Black numbers are density values in 10^3 kg/m^3, white numbers represent magnetic susceptibilities. The black-white dotted line indicates the Curie depth. The red dots mark magnetic sources as calculated by Euler-deconvolution (see Chapter 3.2 of the Ra3 Project report Part 1 for details of analysis). SL indicates the location of the Surt Lineament. See Figs. 2.3 – 2.5, 5.8 & 5.9 for exact location of the section and text for further details.*

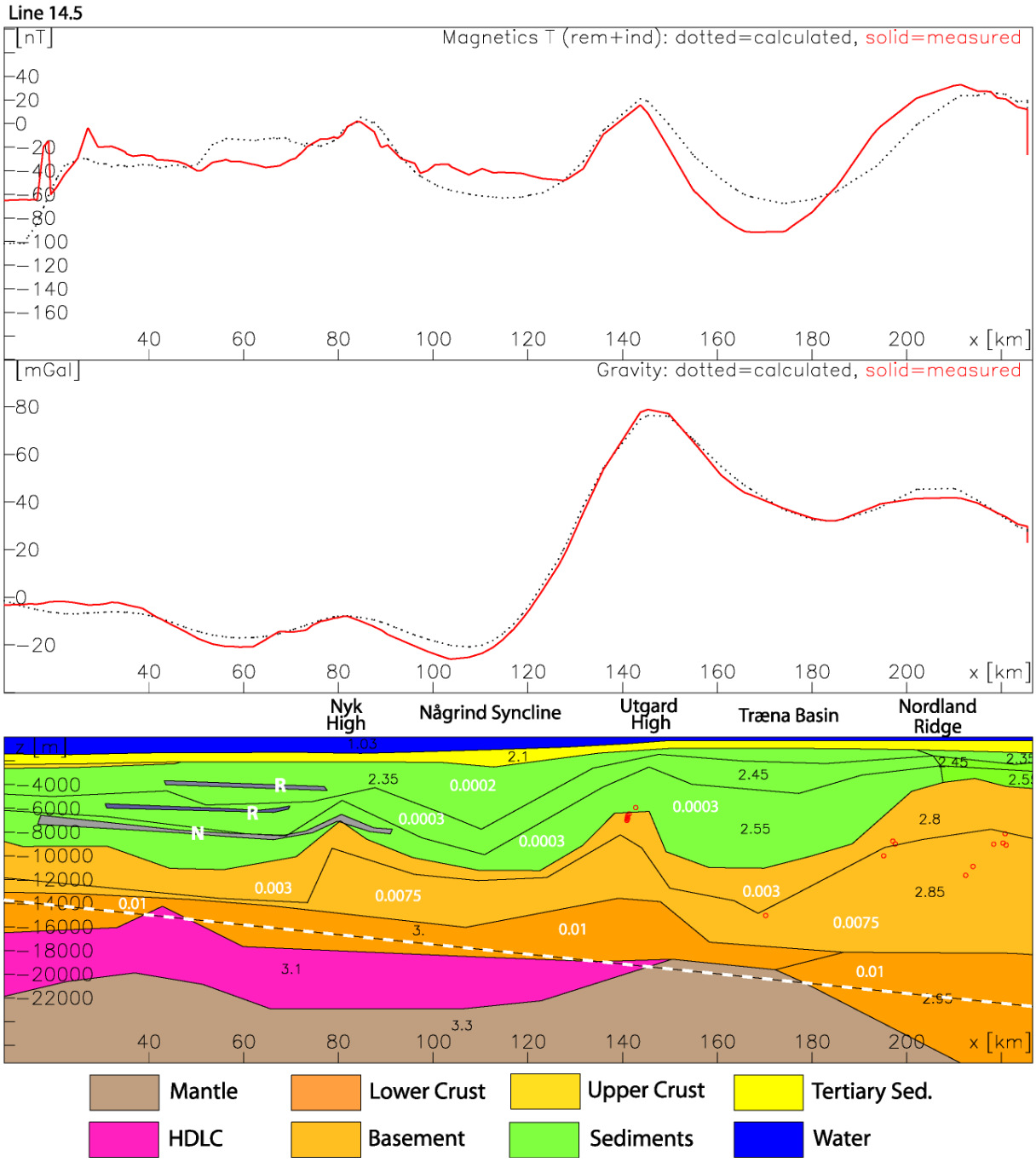

Figure 5.14 *Profile 14.5 of the 3D model. The upper panel shows the magnetic anomaly, the middle panel the gravity anomaly (offshore: Free-air anomaly, onshore: Bouguer anomaly) and the lower panel the modelled density/magnetic cross-section. The grey layers indicate sills with reversed (R) or normal (N) magnetisation. Black numbers are density values in 10^3 kg/m^3, white numbers represent magnetic susceptibilities. The black-white dotted line indicates the Curie depth. The red dots mark magnetic sources as calculated by Euler-deconvolution (see Chapter 3.2 of the Ra3 Project report Part 1 for details of analysis). See Figs. 2.3 – 2.5, 5.8 & 5.9 for exact location of the section and text for further details.*

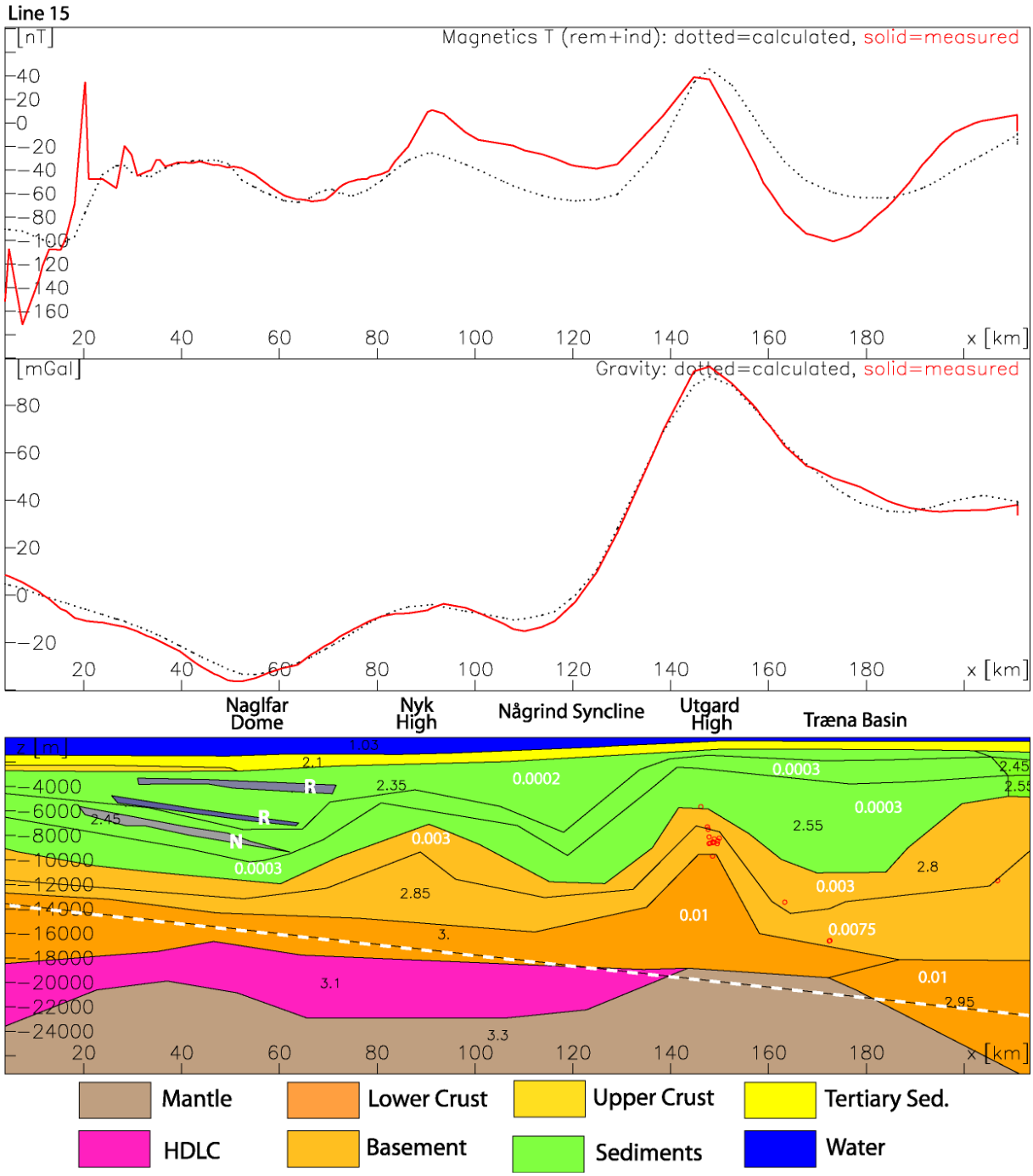

Figure 5.15 *Profile 15 of the 3D model. The upper panel shows the magnetic anomaly, the middle panel the gravity anomaly (offshore: Free-air anomaly, onshore: Bouguer anomaly) and the lower panel the modelled density/magnetic cross-section. The grey layers indicate sills with reversed (R) or normal (N) magnetisation. Black numbers are density values in 10^3 kg/m^3, white numbers represent magnetic susceptibilities. The black-white dotted line indicates the Curie depth. The red dots mark magnetic sources as calculated by Euler-deconvolution (see Chapter 3.2 of the Ra3 Project report Part 1 for details of analysis). SL indicates the location of the Surt Lineament. See Figs. 2.3 – 2.5, 5.8 & 5.9 for exact location of the section and text for further details.*

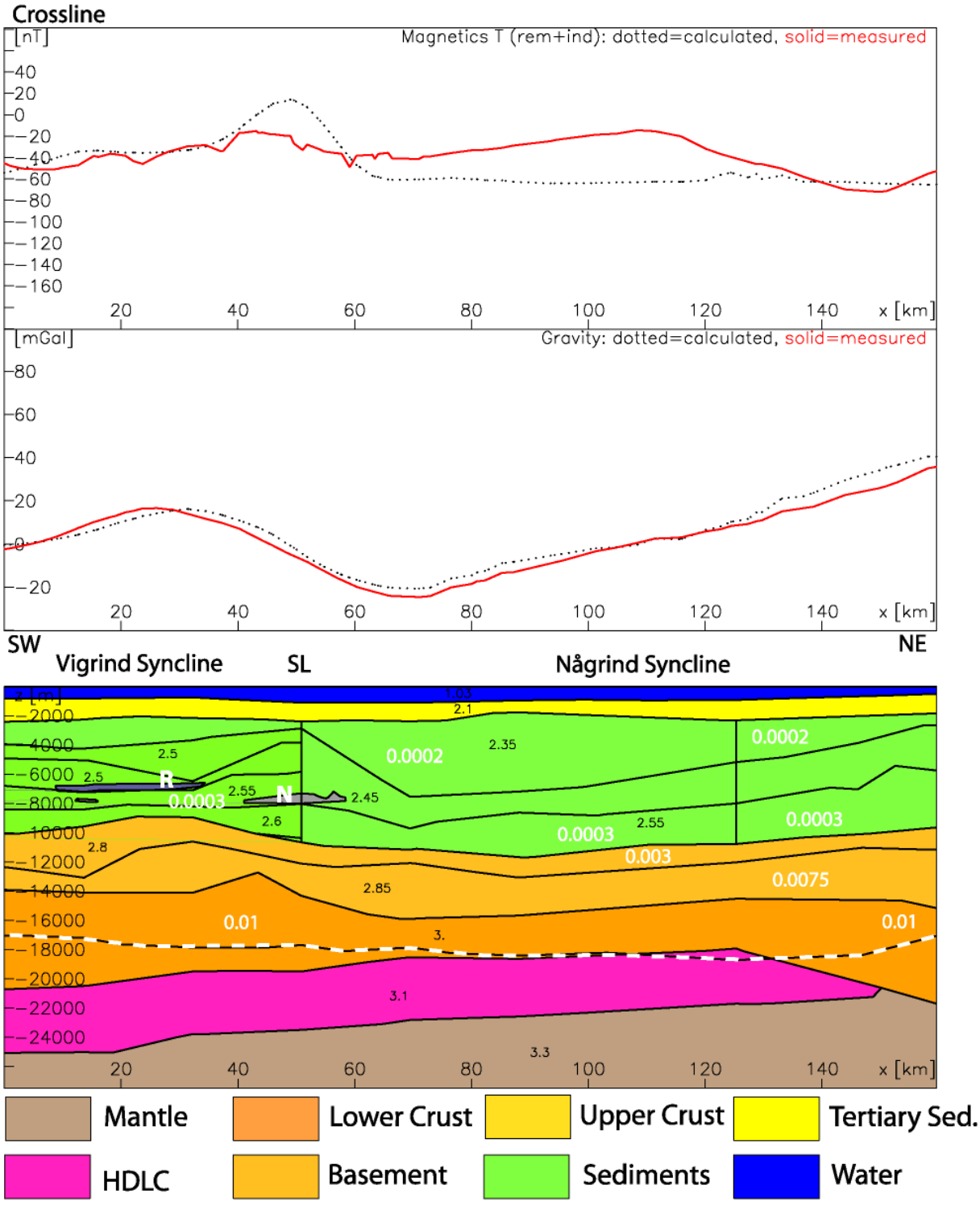

Figure 5.16 *Crossline of the 3D model. The profile is located parallel to and between the Lines 3 (Mjelde et al. 1997) and 7 (Mjelde et al. 1998) of the OBS arrays. For further description see Fig. 5.12. See Figs. 2.3 – 2.5, 5.8 & 5.9 for exact location of the section and text for further details.*

5.3 High-amplitude seismic reflectors and their correlation with magnetic data

On the magnetic map, short wavelength anomalies (Fig. 5.17) occur to the west of the line called 'inner flows', as well as from the Vøring Escarpment and the oceanic crust. In general there is a decrease in pronounced magnetic signature north-eastwards in the Røst Basin.

Seismic line TBN96-115A (Fig. 5.18) represents typical anomalies. To the west of shotpoint 1200 (left in figure), high amplitude reflectors make up 'wavy patterns' from about 4 TWT to 4.4 TWT. These represent flows or sills in the early Tertiary sediments. The magnetic total field (lower discontinuous red curve) and the residual field (upper curve, in blue and red) show anomalies that may result from these intra-sedimentary rocks. We suggest that these represent sills and dykes. This is also in general agreement with Euler depth solutions that show a range of depths (Figs. 3.1-37 in the Ra 3 Part 1 Report, Olesen et al. 2003). Farther to the east (right in figure), a rather smooth high-amplitude reflector is seen from 3.75 TWT to 3.9 TWT. In the east, it terminates against the Sandflesa High/Myken Volcanic Complex.

In line VB-21-89A (Fig. 5.19), the high-amplitude reflectors are less prominent, and the magnetic signal is smoother (see total magnetic field). This change is also reflected in the anomaly map, where the amplitude of the anomalies gradually becomes lower in amplitude north-eastwards in the Røst Basin. The line crosses a lava flow window in the central part of the line. This window has been interpreted by Tsikalas et al. (2001) to represent an area without flows where the underlying tilted sedimentary sequences are visible on the seismic sections. However, a magnetic anomaly is seen that may be due to extrusives. It is possible that these are relatively thin. Only very low amplitudes exist towards the eastern termination of the 'inner flow' (blue line in Fig. 5.17). On the seismic lines, there are only a few examples where an anomaly (of low amplitude) occurs above the eastern part of a basaltic flow that exists at this inner flow boundary. On the western side of the basin, the high amplitude reflectors become more abundant, giving rise to the anomalies seen on the magnetic map. Of course, the most significant anomalies occur near to the Vøring Escarpment, gradually decreasing north-eastwards. However, there is a belt of relatively stronger anomalies towards the Sandflesa high/Myken volcanic complex.

From the analysis we suggest that the western half of the Røst Basin is underlain primarily by intrusions. These sills and dykes are similar in character to intrusions in the area of the Hel Graben, but made up of significant lower volumes. The Euler depths show a range from around 3 km to 5 km (Figs. 3.1-3.7 in the Ra 3 Part 1 Report, Olesen et al. 2003). This is in agreement with the seismic data where a range of depths is seen (edges at different depths). To the north of the Myken Volcanic Complex and the Sandflesa High, only very thin high-amplitude reflectors are seen. However, local feeder systems for these flows may be interpreted. These suggest that the intrusions represent intrabasinal sources for the basalts.

Another possibility is that the line we have drawn as the boundary between sills and flows is a boundary between submarine volcanic rocks and subarial flows.

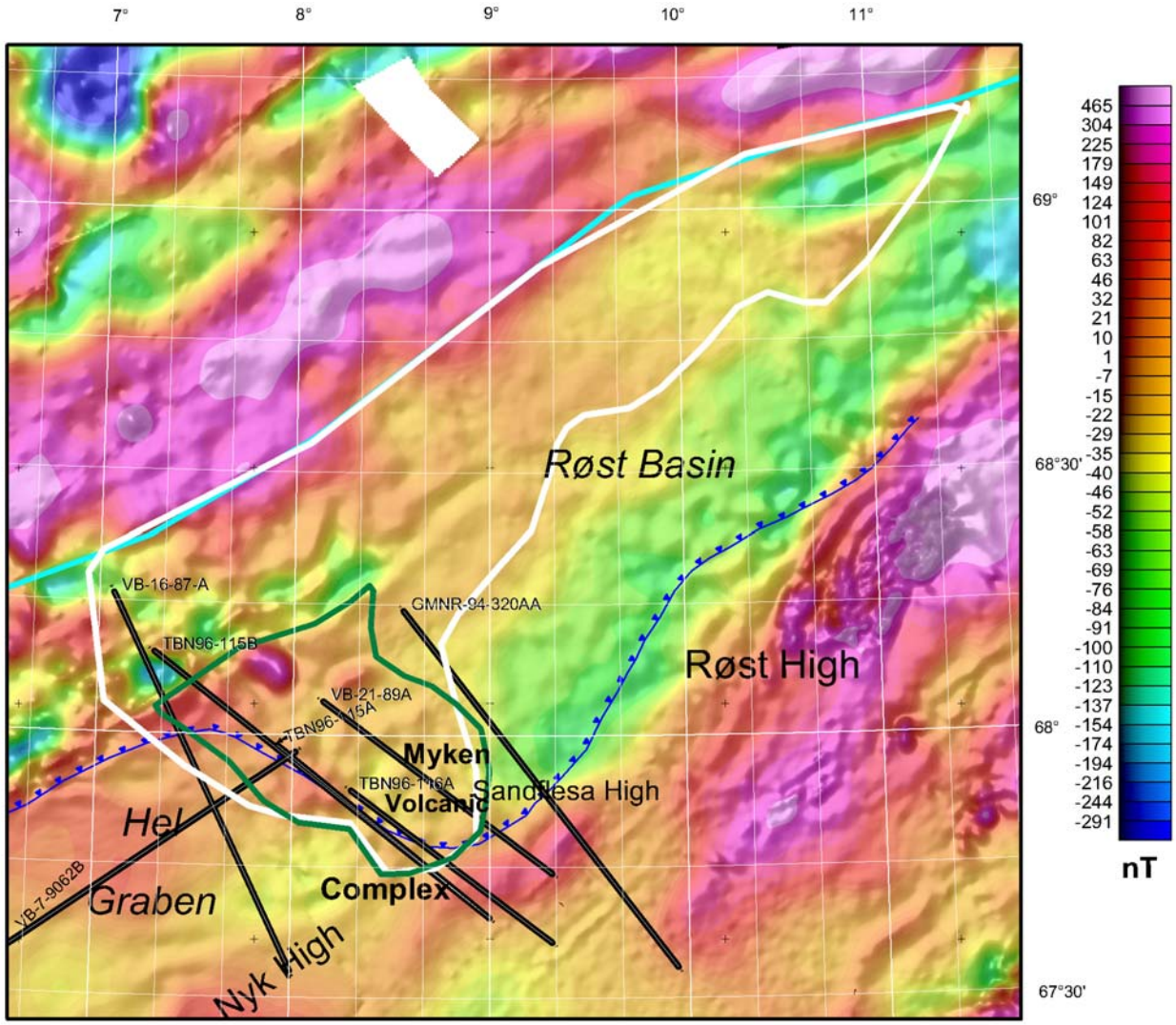

Figure 5.17 *Aeromagnetic map of the Hel Graben – Røst Basin area. A shaded relief version (in grey-tones) of the 25 km high-pass filtered data is superimposed on the total magnetic anomaly map in colours. The studied seismic sections are shown with bold black lines. The four easternmost lines of the studied seismic sections are shown in the present report (Figs. 5.18-5.21). The thin and dark blue line shows the easternmost termination of the flow basalts (from Blystad et al. (1995) and T. Henningsen pers. com. 2003). The green line includes the area with the most intense magmatism while the white line depicts the area affected by sill intrusions in the western part of the Røst Basin. See Fig. 5.7 for legend.*

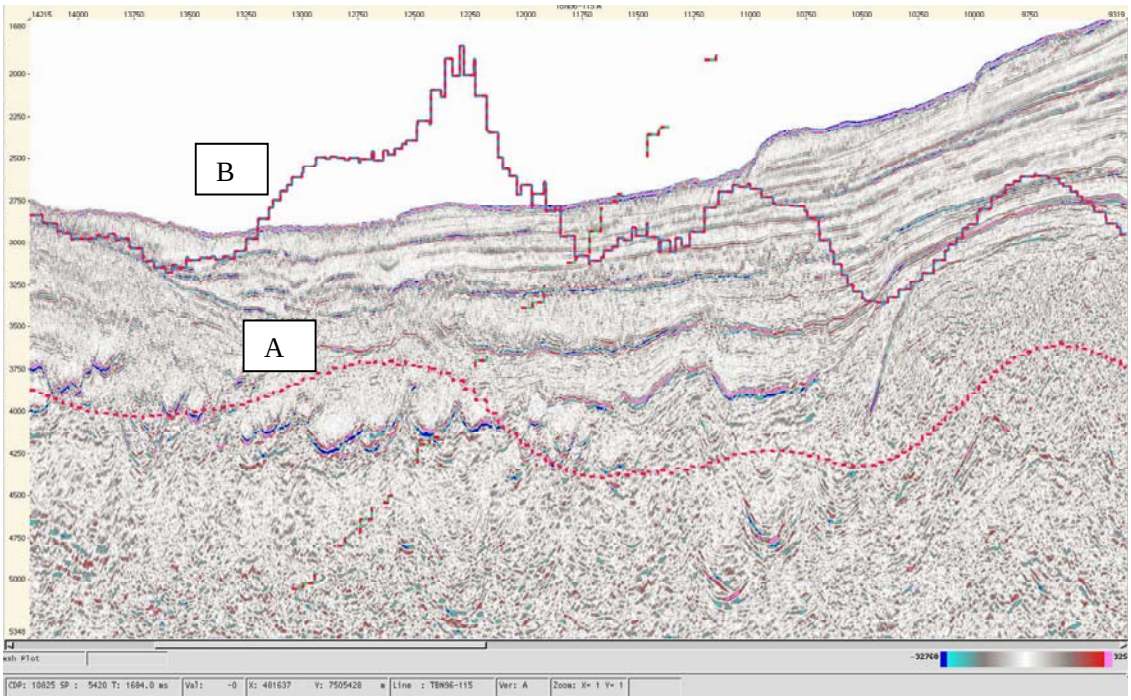

Figure 5.18 *Seismic line TBN96115A. Left is to the northwest, and right is to the southeast. The lower curve (A, in red) is total magnetic field, upper curve B is residual magnetic field. Note wavy high-amplitude reflectors between 4000 ms TWT and 4500 ms TWT, which give rise to magnetic anomalies. These may represent sills.*

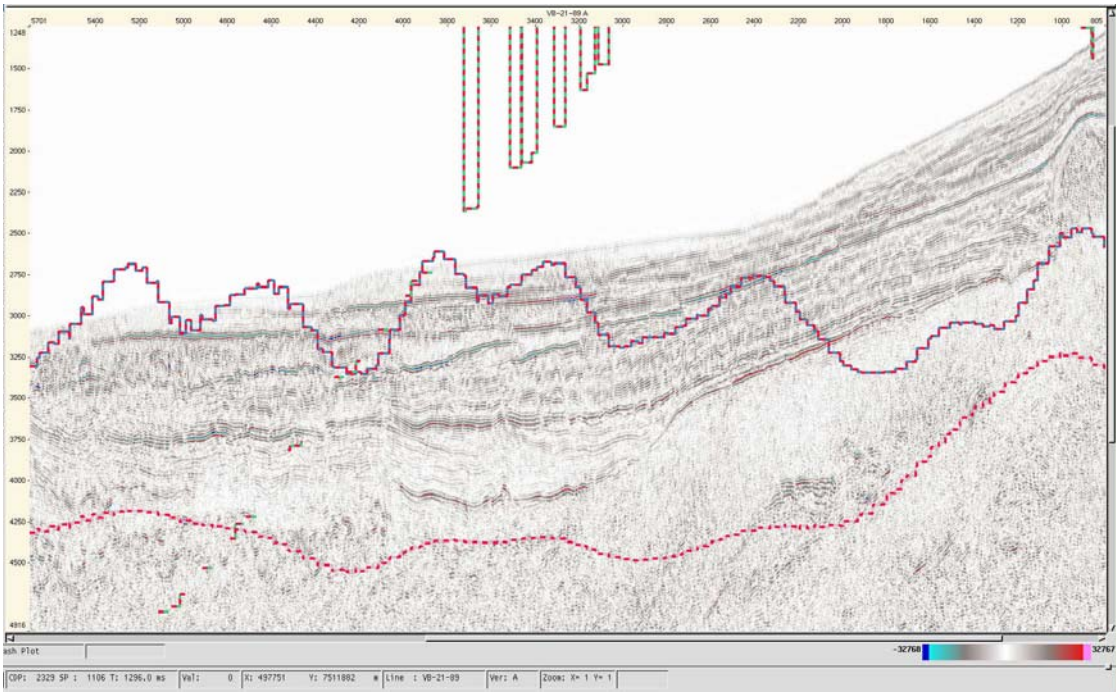

Figure 5.19 *Seismic line VB-21-89A. Left is northwest, and right is southeast. The lower curve (red) is total magnetic field, upper curve is residual magnetic field. Anomalies probably relate to intrusions (western part) and to extrusives seen in the central part of the line. Because the volumes of volcanic rocks change laterally, magnetic anomalies are also rather chaotic in character. Note that the high-amplitude reflectors occur below 4000 ms TWT.*

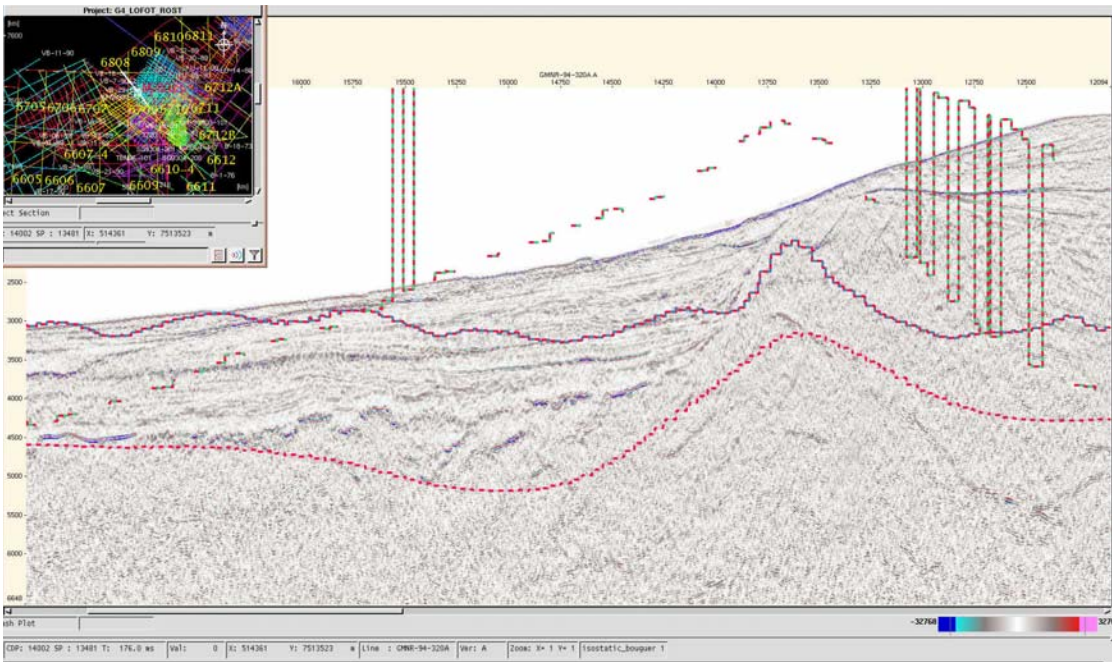

Figure 5.20 *Seismic line GMNR-94-320AA. Left is northwest, and right is southeast. The lower curve (red) is total magnetic field, middle curve is residual magnetic field, upper curve (with some noise) is gravity. Anomalies probably relate to both intrusives and extrusives. Because the volumes of volcanic rocks change laterally, magnetic anomalies are also rather chaotic in character. Note that the high-amplitude reflectors occur below 4000 ms TWT, and the very small magnetic signal.*

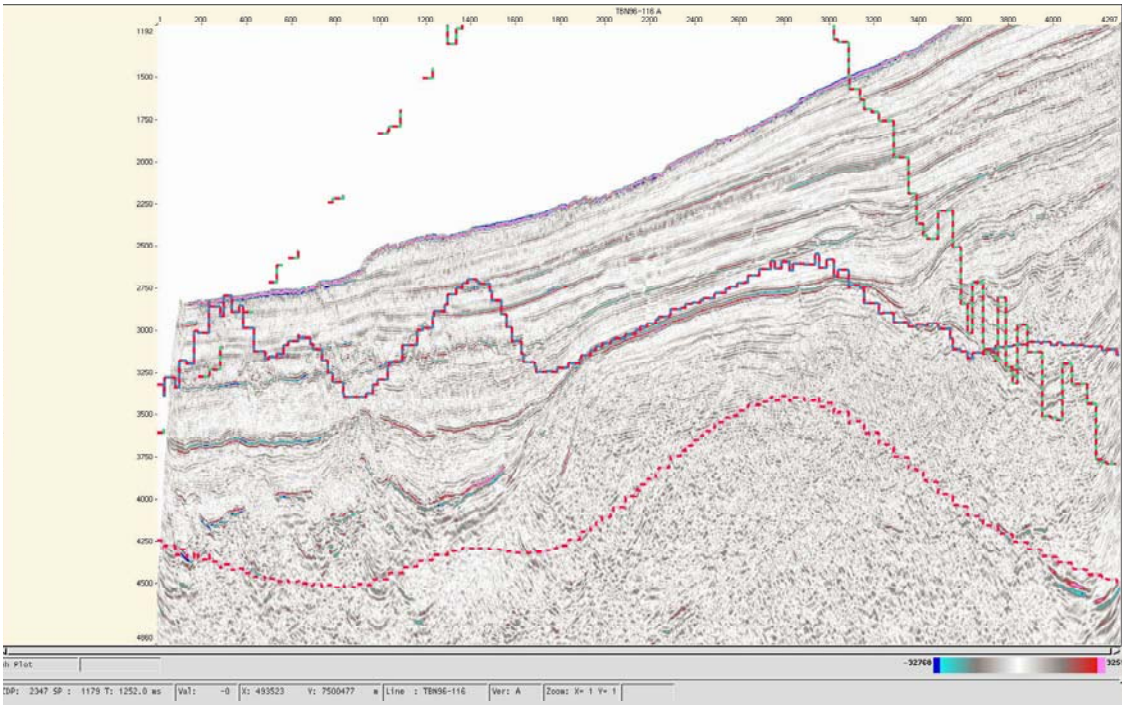

Figure. 5.21 *Seismic line TBN96-116A. Left is northwest, and right is southeast. The lower curve (in red) is total magnetic field, middle curve B is residual magnetic field. Erratic line is gravity. Note high-amplitude reflectors between 4000 ms TWT and 4500 ms TWT, that give rise to anomalies.*

6. CONCLUSIONS

1. The opening of the Norwegian-Greenland Sea (between the Jan Mayen and Senja fracture zones) occurred along stable continental margins without offsets of oceanic spreading anomalies or jumps in spreading axis. This interpretation deviates significantly from earlier interpretations with reported offsets of up to 50 km (e.g. Hagevang et al. 1983, Blystad et al. 1995, Tsikalas et al. 2001, 2002, Olesen et al. 2002). The previously proposed offset zones were merely artefacts of wide profile spacing, poor navigation and poor profile levelling of the vintage aeromagnetic profiles.

2. Palaeogeographic reconstruction of the aeromagnetic map to Anomaly 22 reveals that a c. 50 km wide igneous complex cut across spreading anomalies 24A, 24B and 23 from the Vøring Marginal High on the Norwegian margin to the island Traill Ø on the Greenland coast. The postulated igneous complex cuts across anomaly 22 on the Greenland margin, revealing that the igneous activity was active at least until c. 50 Ma. The magnetic response of this complex along the Vøring margin has earlier been interpreted to represent spreading anomalies 24A and 24B. This interpretation in turn introduced the need to invoke an abandoned spreading ridge and the Gleipne Fracture Zone in this area.

3. 3D modelling reveals that the Surt Lineament is not a regional tectonic boundary of same importance as the Bivrost Lineament. There are minor differences in basin depths across the lineament, but it does not separate basement rocks with different physical parameters.

4. The western half of the Røst Basin is heavily intruded by mafic sills. Combined interpretation of reflection seismic and potential field data reveals that the sills and dykes resemble the Hel Graben intrusions. To the north of the Myken Volcanic Complex and the Sandflesa High, only very thin high-amplitude reflectors (intrusions) are seen. However, local feeder systems for these flows may be interpreted. These suggest that the intrusions represent intrabasinal sources for the basalts.

5. Part 1 of the Ra 3 Project showed that the structural setting of the Utgard High resembles the Lofoten Ridge with large-scale normal faults on either side and a shallow underlying Moho caused by overlapping zones of uniform crustal thinning at depth. Two basement highs, Sandflesa and Flakstad, occur along the western boundary of the Utrøst Ridge at a depth of approximately 6 km.

6. The closer line spacing of the RAS-03 aeromagnetic profiles compared with the old NGU-73 and NRL-73 surveys has provided a more detailed image of the magnetic sources in the Røst Basin area.

7. RECOMMENDATIONS FOR FURTHER WORK

1. The success of the present study in delineating the regional tectonic setting along the Lofoten continental margin, especially in locating the magnetic spreading anomalies, leads us to recommend similar investigations along the East Jan Mayen Fracture Zone, on the Møre Marginal High and along the western margin of the north and central Barents Sea (Fig. 2.1) where the profile coverage is poor. The aeromagnetic data in the southeastern Barents Sea were acquired in the early 1970s using Decca navigation and should also be replaced by modern high-resolution data. Pre-1980 seismic data are today regarded as obsolete and are very seldom used for detailed interpretations. Based on the Ra 3 results we conclude that the same problems apply to the pre-1980 aeromagnetic surveys.

2. We will carry out a 3D modelling of the East Greenland continental shelf using the NRL and GEUS aeromagnetic profiles, satellite gravity data and available seismic data. Wide spacing (10 - 20 km) of the aeromagnetic profiles (Fig. 5.8) inhibits the application of the Euler 3D depth estimate method (grid-based method). Therefore, we suggest using a combination of the Naudy (1971) method on the aeromagnetic profiles and a forward 3D modelling of parallel aeromagnetic and gravity lines extracted from the original aeromagnetic profiles and gravity grid. This approach will facilitate a continuous depth to basement map across the reconstructed East Greenland - Mid Norwegian continental margins as shown in Fig. 5.8.

8. ACKNOWLEDGEMENTS

BP Norge, Norsk Hydro, Statoil, NPD and NGU financed the Røst Aeromagnetics 2003 Project (Ra 3). Evan Kåre Hansen and Bjørn Træet (BP Norge), Jan Nordås and Peter Midbøe (Norsk Hydro), Morten Sand and Tore Høy (NPD), Tormod Henningsen and Oddbjørn Kløvjan (Statoil) gave advice during the project period. Morten Sand and Tore Høy assisted in loading the potential field data into the computer at NPD to facilitate the joint interpretation with seismic data using the Geoframe Charisma software package. We express our sincere thanks to these companies, institutions and persons.

9. REFERENCES

Amarok 1995: Processing Report on VGVB-94. Amarok Internal Report, 18 pp.

Andresen, A. & Forslund, T. 1987: Post-Caledonian brittle faults in Troms: geometry, age and tectonic significance. *The Caledonian and related geology of Scandinavia* (Cardiff, 22-23 Sept., 1989) (Conf. abstr.).

Berndt, C., Skogly, O.P., Planke, S., Eldholm, O. & Mjelde, R. 2000: High-velocity breakup-related sills in the Vøring Basin, off Norway. *Journal of Geophysical Research 105*, 28.443-28.454.

Berndt, C., Planke, S., Alvestad, E., Tsikalas, F. & Rasmussen, T. 2001: Seismic volcanostratigraphy of the Norwegian Margin: constraints on tectonomagmatic brek-up processes. *Journal of the Geological Society, London 158,* 413-426.

Blystad, P., Brekke, H., Færseth, R.B., Larsen, B.T., Skogseid, J. & Tørudbakken, B. 1995: Structural elements of the Norwegian continental shelf, Part II. The Norwegian Sea Region. *Norwegian Petroleum Directorate Bulletin 8,* 45 pp.

Brekke, H. 2000: The tectonic evolution of the Norwegian Sea continental margin with emphasis on the Vøring and Møre basins. *In* Nøttvedt, A. et al. (eds.) *Dynamics of the Norwegian Margin.* Geological Society of London, Special Publication 167, 327-378.

Brekke, H. & Riis, F. 1987: Tectonics and basin evolution of the Norwegian shelf between 62^{o} and 72^{o}N. *Norsk Geologisk Tidsskift 67,* 295-322.

Braathen, A., Nordgulen, Ø., Osmundsen, P.T., Andersen, T.B., Solli, A. & Roberts, D. 2000: Devonian, orogen-parallel, opposed extension in the Central Norwergian Caledonides. *Geology 28,* 615-618.

Braathen, A., Osmundsen, P.T., Nordgulen, Ø. & Roberts, D. 2002: Orogen-parallel, extensional denudation of the Caledonides in North Norway. *Norsk Geologisk Tidsskrift 82*, 225-241.

Breunig, M., Cremers, A.B., Götze, H.-J., Schmidt, S., Seidemann, R., Shumilov, S. & Siehl, A. 2000: Geological Mapping based on 3D models using an Interoperable GIS. Geo-Information-Systems. Journal for Spatial Information and Decision Making 13, 12-18.

Cande, S.C. & Kent, D.V. 1995: Revised calibration of the geomagnetic polarity timescale for the Late Cretaceous and Cenozoic. *Journ. Geophys. Res. 100,* 6093-6095.

Cox, A. & Hart, R.B. 1986: *Plate tectonics. How it works.* Blackwell Scientific Publications 381 pp.

Desmond Fitzgerald and Associates 1996: INTREPID Geophysical processing and visualisation tools reference manual Vol. 2, *241 pp.*

Doré, A.G., Lundin, E.R., Jensen, L.N., Birkeland, Ø., Eliassen, P.E. & Fichler, C. 1999: Principal tectonic events in the evolution of the northwest European Atlantic margin. In: Fleet, A.J. and Boldy, S.A.R. (eds.) *Petroleum Geology of Northwest Europe: Proceedings of the 5th conference.* Geological Society, London, 41-61.

Ebbing, J. 2004: Gravity and magnetic interpretation of the regional deep structure of the Vøring Basin. *NGU Report 2003.81,* 41pp.

Eldholm, O. & Grue, K. 1994: North Atlantic volcanic margins; dimensions and production rates. *Journal of Geophysical Reserach B,* 99, 2955-2968.

Eldholm, O., Sundvor, E. & Myhre, A. 1979: Continental margin off Lofoten-Vesterålen, Northern Norway. *Marine Geophysical Research 4,* 3-35.

Eldholm, O., Tsikalas, F. & Faleide, J.I. 2002: The continental margin off Norway 62-75ºN: Palaeogene tectono-magmatic segmentation and sedimentation. In: D. Jolley & B. Bell (eds.). The North Atlantic Igneous Province: stratigraphy, tectonics, volcanic and magmatic processes. *Geological Society, London, Special Publication 197,* 39-68.

Escher, J.C. & Pulvertaft, T.C.R. 1995. *Geological map of Greenland,* 1:2,500,000. Copenhagen: Geological Survey of Greenland.

Fichler, C., Rundhovde, E., Olesen, O., Sæther, B.M., Rueslåtten, H., Lundin, E. & Doré, A.G. 1999: Regional tectonic interpretation of image enhanced gravity and magnetic data covering the Mid-Norwegian shelf and adjacent mainland. *Tectonophysics 306,* 183-197.

Gernignon, L., Ringenbach, J.-C., Planke, S. and Le Gall, B. 2002: Crustal structure and rifting along volcanic rifted margins: the Vøring Margin (Mid-Norway). In: Jónsson, S.S. (ed.): 25th Nordic Geological Winter Meeting, Abstract Volume, 61.

Gernignon, L., Ringenbach, J.C., Planke, S., Le Gall, B. & Jonquet-Kolstø, H. 2003: Extension, crustal structure and magmatism at the outer Vøring Basin, Norwegian margin. *Journal of the Geological Society, London 160,* 197-208.

Geosoft 2000a: Geosoft GridKnit, Grid stitching tool for OASIS Montaj, Tutorial and user guide, Geosoft Incorporated, 28 pp.

Geosoft 2000b: MAGMAP (2D-FFT), 2-D frequency domain processing of potential field data, Geosoft Incorporated, 67 pp.

Geosoft 2001: OASIS Montaj v 5.1, The core software platform for working with large volume spatial data. Data Processing System for Earth Sciences Applications. Users manual, Geosoft Incorporated, 228 pp.

Götze, H.-J. & Lahmeyer, B. 1988: Application of three-dimensional interactive modeling in gravity and magnetics. *Geophysics 53,* 1096-1108.

Hagevang, T., Eldholm, O. & Aalstad, I. 1983: Pre-23 magnetic anomalies between Jan Mayen and Greenland-Senja Fracture Zones in the Norwegian Sea. *Marine Geophysical Researches 5,* 345-363.

Hartz, E.H., Eide, E.A., Andresen, A., Midbøe, P., Hodges, K.V. & Kristiansen, S.N. 2002: $^{40}Ar/^{39}Ar$ geochronology and structural analysis: Basin evolution and detrital feedback mechanisms, Hold With Hope region, East Greenland. *Norsk Geologisk Tidsskrift 82,* 341-358.

Heiskanen, W.A. & Moritz, H. 1967: Physical Geodesy. *W.H. Freeman, San Fransisco.* 364 pp.

Hunt, C., Moskowitz, B.M. & Banerje, S.K. 1995: Magnetic properties of rocks and minerals. In: Rock Physics and Phase Relations. A Handbook of Physical Constraints. *AGU Reference Shelf 3,* 189-204.

Kinck, J.J., Husebye, E.S. & Larsson, F.R. 1993: The Moho depth distribution in

Fennoscandia and the regional tectonic evolution from Archean to Permian times, *Precambrian Research 64,* 23-51.

Larsen, H.C. 1988: A multiple and propagating rift model for the NE Atlantic. In: Morton, A.C. & Parson, L.M. (eds.). *Early Tertiary Volcanism and the Opening of the NE Atlantic*. *Geological Society, London, Special Publications 39,* 157-158.

Larsen, H.C. 1990: The East Greenland Shelf. *The Geology of North America, The Arctic Ocean region,* Vol. L, The Geological Society of America, 185-209.

Ludwig; J.W., Nafe, J.E. & Drake, C.L. 1970: Seismic refraction. In: Maxwell., A. (ed.): *The sea, Vol.4* Wiley, New York.

Lund, C-E. 1979: Crustal structure along the Blue Road Profile in northern Scandinavia. *Geologiska Föreningens i Stockholm Förhandlingar 101,* 191-204.

Lundin, E.R. & Doré, A.G. 1997: A tectonic modell for the Norwegian passive margin with implications for the NE Atlantic: Early Cretaceous to break-up. *The Geological Society, London, Special Publications 1584,* 545-550.

Lundin, E.R., Rønning, K., Doré, A.G. &. Olesen O. 2002: Hel Graben, Vøring Basin, Norway – a possible major cauldron? Abstract, 25th Nordic Geological Winter Meeting, January 6th - 9th , 2002, Reykjavik.

Lundin, E.R. 2002: Atlantic – Arctic seafloor spreading history. In: Eide, E. A. (coord.), *BATLAS – Mid Norway plate reconstructions atlas with global and Atlantic perspectives*. Geological Survey of Norway, 40-47.

Lundin, E.R., Torsvik, T.H., Olesen, O. & Roest, W.R. 2002: The Norwegian Sea, a meeting place for opposed and overlapping Arctic and Atlantic rifts; implications for magmatism. AAPG Hedberg Conference "*Hydrocarbon Habitat of Volcanic Rifted Passive Margins*", September 8-11, 2002, Stavanger, Norway.

Lundin, E.R. & Doré, A.G. in press: NE-Atlantic break-up: a re-examination of the Iceland mantle plume model and the Atlantic –Arctic linkage. In: Doré, A.G. & Vining, B.A. (eds.) *North-West European Petroleum Geology and Global Perspectives: Proceedings of the 6th Conference.* Geological Society, London.

Løseth, H. & Tveten, E. 1996: Post-Caledonian structural evolution of the Lofoten and Vesterålen offshore and onshore areas. *Norsk Geologisk Tidsskrift 76,* 215-230.

Mauring, E., Smethurst, M.A. & Kihle, O. 1999: Vestfjorden Aeromagnetic Survey 1998. Acquisition and processing report. *NGU Report 99.001,* 23 pp.

Mauring, E., Beard, L.P., Kihle, O. & Smethurst, M.A. 2002: A comparison of aeromagnetic levelling techniques with an introduction to median levelling. *Geophysical Prospecting 50,* 43-54.

Mauring, E., Mogaard, J.O. & Olesen, O. 2003: Røst Basin Aeromagnetic Survey 2003 (RAS-03). Ra 3 aeromagnetic compilation. Data acquisition and processing report. NGU Report 2003.070, 20 pp.

Mjelde, R., Sellevoll, M.A., Shimamura, H., Iwasaki, T. & Kanazawa, T. 1992: A crustal study off Lofoten, N.Norway, by use of 3-component ocean bottom seismographs. *Tectonophysics 212,* 269-288.

Mjelde, R., Sellevoll, M.A., Shimamura, H., Iwasaki, T. & Kanazawa, T. 1993: Crustal

structure beneath Lofoten, N.Norway, from vertical incidence and wide-angle seismic data. *Geophysical Journ. Int. 114,* 116-126.

Mjelde, R., Kodaira, S., Shimamura, H., Kanazawa, T. Shiobara, H., Berg, E.W. & Riise, O. 1997: Crustal structure of the central part of the Vøring Basin, mid-Norway margin, from ocean bottom seismographs. *Tectonophysics 277,* 235-257.

Mjelde, R., Digranes, P., Shimamura, H., Shiobara, H., Kodaira, S., Brekke, H., Egebjerg, T., Sørenes, N. & Thorbjørnsen, S. 1998: Crustal structure of the northern part of the Vøring Basin, mid-Norway margin, from wide-angle seismic and gravity data. *Tectonophysics 293,* 175-205.

Mjelde, R., Digranes, P., van Schaack, M., Shimamura, H., Shiobara, H., Kodaira, S. & Næss O. 2001. Crustal structure of the outer Vøring Plateau, offshore Norway, from ocean bottom seismic and gravity data. *Journal of Geophysical Research 106,* 6769-6791.

Mjelde, R., Raum, T., Digranes, P., Shimamura, H., Shiobara, H. & Kodaira, S. 2003a: V_p/V_s ratio along the Vøring Margin, NE Atlantic, derived from OBS data: implications on lithology and stress field. *Tectonophysics 369,* 175-197.

Mjelde, R., Shimamura, H., Kanazawa, T., Kodaira, S., Raum T. & Shiobara, H. 2003b: Crustal lineaments, distribution of lower crustal intrusives and structural evolution of the Vøring Margin, NE Atlantic; new insight from wide-angle seismic models. *Tectonophysics 369,* 199-218.

Mjelde, R., Iwasaki, T., Shimamura, H., Kanazawa, T., Kodaira, S., Raum, T. & Shiobara, H. 2003c: Spatial relationship between recent compressional structures and older high-velocity crustal structures; examples from the Vøring Margin, NE Atlantic, and Northern Honshu, Japan. *Journal of Geodynamics 36-4,* 537-562.

Mokhtari, M. & Pegrum, R.M. 1992: Structure and evolution of the Lofoten continental margin, offshore Norway. *Norsk Geologisk Tidsskrift 72,* 339-355.

Mosar, J. Torsvik, T.H. & the BAT team 2002: Opening of the Norwegian and Greenland Seas: Plate tectonics in Mid Norway since the Late Permian. *In:* Eide, E.A. (coord.), *BATLAS – Mid Norway plate reconstruction atlas with global and Atlantic perspectives.* Geological Survey of Norway. pp. 48-59.

Mørk M.B.E., McEnroe, S.A. & Olesen, O. 2002: Magnetic susceptibility of Mesozoic and Cenozoic sediments off Mid Norway and the role of siderite: implications for interpretation of high-resolution aeromagnetic anomalies. *Marine and Petroleum Geology 19,* 1115-1126.

Naudy, H. 1971: Automatic determination of depth on aeromagnetic profiles. *Geophysics 36,* 717-722.

Nielsen, T.F.D. 1987: Tertiary alkaline magmatism in East Greenland: a review. In: Fitton, J.G. & Upton, B.G.J. (eds.), *Alkaline Igneous Rocks, Geological Society, London, Special Publications 30,* 489-515.

Nielsen, T.F.D. 2002: Palaeogene intrusions and magmatic complexes in East Greenland, 66 to 75°N. *Geological Survey of Denmark and Greenland Report 2002/113,* 249 pp.

Noble, R.H., Macintyre, R.M. & Brown, P.E. 1988: Age constraints on Atlantic evolution: timing of magmatic activity along the E Greenland continental margin. In: Morton,

A.C. & Parson, L.M. (eds.), *Early Tertiary Volcanism and the Opening of the NE Atlantic*. Geological Society, London, Special Publications 39, 201-214.

Nordgulen, Ø., Braathen, A., Corfu, F., Osmundsen, P.T. & Husmo, T. 2002: Polyphase kinematics and geochronology of the late-Caledonian Kollstraumen detachment, north-central Norway. *Norsk Geologisk Tidsskrift 82,* 299-316.

Norges geologiske undersøkelse 1992: Aeromagnetisk anomalikart, Norge M 1:1 mill, Norges geologiske undersøkelse.

Nunns, A.G. 1983. Plate tectonic evolution of the Greenland-Scotland Ridge and surrounding regions. In: Bott, M.H.P., Saxov, S., Talwani, M. & Thiede, J. (eds.). *Structure and Development of the Greenland-Scotland Ridge*: New Methods and Concepts. Plenum Press, New York, 11-30.

Olesen, O. & Myklebust, R. 1989: LAS-89, Lofoten Aeromagnetic Survey 1989, Interpretation report. *NGU Report 89.168,* 54 pp.

Olesen, O. & Torsvik, T.H. 1993: Interpretation of aeromagnetic and gravimetric data from the Lofoten-Lopphavet area. *NGU Report 93.032,* 77 pp.

Olesen, O. & Smethurst, M.A. 1995: NAS-94 Interpretation Report, Part III: Combined interpretation of aeromagnetic and gravity data. *NGU Report 95.040,* 50 pp.

Olesen, O., Torsvik, T.H., Tveten, E., Zwaan, K.B., Løseth H. & Henningsen, T. 1997: Basement structure of the continental margin in the Lofoten-Lopphavet area, northern Norway: constraints from potential field data, on-land structural mapping and palaeomagnetic data. *Nor. Geol. Tidsskr. 77,* 15-33.

Olesen, O., Lundin, E., Nordgulen, Ø., Osmundsen, P.T., Skilbrei, J.R., Smethurst, M.A., Solli, A., Bugge, T. & Fichler, C. 2002: Bridging the gap between the onshore and offshore geology in Nordland, northern Norway. *Norwegian Journal of Geology 82,* 243-262.

Olesen, O., Ebbing, J., Skilbrei, J.R. & Lundin, E. 2003: Interpretation of potential field data along the Lofoten continental margin, Part I. *NGU Report 2003.070,* 68 pp.

Osmundsen, P.T., Braathen, A., Nordgulen, Ø., Roberts, D., Meyer, G.B. & Eide, E. 2003: The Devonian Nesna shear zone and adjacent gneiss-cored culminations, North-central Norwegian Caledonides. *Journal Geol. Soc. London 160,* 1-14.

Phillips, J.D. 1979: ADEPT: A program to estimate depth to magnetic basement from sampled magnetic profiles. *U.S. Geological Survey open-file report 79-367,* 35 pp.

Planke, S., Alvestad, E. & Eldholm, O. 1999: Seismic characteristics of basaltic extrusive rocks. *The Leading Edge 18,* 342-348.

Roberts, D.G., Thompson, M., Mitchener, B., Hossack, J., Carmichael, S. & Bjørnseth, H.-M. 1999: Palaeozoic to Tertiary rift and basin dynamics: mid-Norway to the Bay of Bicsay – a new context for hydrocarbon prospectivity in the deep water frontier. In: Fleet, A.J. & Boldy, S.A.R. (eds.), *Petroleum Geology of Northwest Europe*: Proceedings of the 5th Conference, Geological Society of London, 7-40.

Rykkelid, E. & Andresen, A. 1994: Late Caledonian extension in the Ofoten area, northern Norway. *Tectonophysics 231,* 157-169.

Schmidt, S. & Götze, H.-J., 1998: Interactive visualization and modification of 3D models

using GIS functions. *Phys. Chem. Earth 23*, 289-296.

Scott, R.A. 2000: Mesozoic-Cenozoic evolution of East Greenland: Implications of a reinterpreted continent-ocean boundary location. *Polarforschung 68,* 83-91.

Sellevoll, M.A. 1983: A study of the Earth in the island area of Lofoten- Vesterålen, northern Norway. *Norges geologiske undersøkelse 380,* 235-243.

Simpson, R.W., Jachens, R.C., & Blakely, R.J. 1983: AIRYROOT: A Fortran program for calculating the gravitational attraction of an Airy isostatic root out to 166.7 km. *United States Department of the Interior, Geological Survey, Open-File Report 83-883,* 24 pp.

Skilbrei, J.R., Olesen, O., Osmundsen, P.T., Kihle, O., Aaro, S. and Fjellanger, E., 2002. A study of basement structures and onshore-offshore correlations in Central Norway. *Norsk Geologisk Tidsskrift 82,* 263-279.

Skogseid, J. & Eldholm, O. 1987. Early Cenozoic crust at the Norwegian continental margin and the conjugate Jan Mayen Ridge. *Journal of Geophysical Research 92,* 11471-11491.

Skogseid, J., Pedersen, T., Eldholm, O. & Larsen, B.T. 1992: Tectonism and magmatism during NE Atlantic continental break-up: the Vøring margin. In: Story, B.C., Alabaster, T. & Plankhurst, R.J. (eds.), Magmatism and the causes of continental break-up. *Geological Society of London, Special Publication 68,* 305-320.

Steltenpohl, M.G., Hames, W.E. & Andresen, A. 2004: The Silurian to Permian history of a metamorphic core complex in Lofoten, northern Scandinavian Caledonides. *Tectonics 23,* TC1002, 1-23

Talwani, M. & Eldholm, O. 1977: Evolution of the Norwegian-Greenland Sea. *Geological Society of America Bulletin 88,* 969-999.

TGS-Nopec 2000: High-Density Aeromagnetic Survey, VBEAM-00, at Outer Vøring Basin, Norwegian Sea, Processing Report , 19 pp.

Thompson, D.T., 1982. EULDPH: A new technique for making computer-assisted depth estimates from magnetic data. *Geophysics 47,* 31-37.

Torsvik, T.H., Mosar, J. & Eide, E.A. 2001: Cretaceous-Tertiary geodynamics: a North Atlantic exercise. *Geophysical Journal International 146,* 850-866.

Tsikalas, F., Faleide, J.I. & Eldholm, O. 2001: Lateral variations in tectono-magmatic style along the Lofoten-Vesterålen volcanic margin off Norway. *Marine and Petroleum Geology 18,* 807-832.

Tsikalas, F., Eldholm, O. & Faleide, J.I. 2002: Early Eocene sea floor spreading and continent-ocean boundary between Gleipne and Senja fracture zones in Norwegian-Greenland Sea. *Marine Geophysical Researches 23,* 247-270.

Verhoef, J., Roest, W.R., Macnab, R., Arkani-Hamed, J. & Members of the Project Team 1996: Magnetic anomalies of the Arctic and North Atlantic Oceans and adjacent land areas. *GSC Open File 3125, Parts a and b* (CD-ROM and project report), Geological Survey of Canada, Dartmouth NS.

Vink, G.E. 1984. A hotspot model for Iceland and the Vøring Plateau. *Journal of Geophysical Research 89, B12,* 9949-9959.

List of figures and tables

Figures

Figure. 5.21 Seismic line TBN96-116A.

Tables

Table 2.1. Offshore aeromagnetic surveys compiled for the present study (Figs. 2.1 & 2.4). The RAS-03 survey included 2.300 km reflying of the LAS-89 survey.

Table 2.2 Aeromagnetic grids (500 x 500 m) included in the regional compilation. The Gammaa5 compilation (5 x 5 km grid) by Verhoef et al. (1996) from the Norwegian-Greenland Seas was regridded to a 500x500m grid and included in the regional compilation (Figs. 2.1 &- 2.4).

Table 3.1. Euler rotation parameters used to restore Greenland back to its 49.7 and 54.0 Ma positions relative to Europe.